23. NATURAL GAMMA RADIATION OF SEDIMENTS FROM THE WESTERN EQUATORIAL PACIFIC: LEG 7, *GLOMAR CHALLENGER*

E. L. Gealy, Scripps Institution of Oceanography, La Jolla, California

INTRODUCTION

The distribution of radionuclides with depth in marine sediments is poorly understood, and the study of the gamma radiation cores of sediments recovered by deep ocean drilling could provide a unique opportunity for studying some aspects of this distribution.

The D/V *Glomar Challenger* is equipped with a system wherein the total gamma rays emitted over a given period by cores are counted and recorded. Unfortunately, the system is a relatively "noisy" one, it has not been rigorously calibrated; and, it does not permit determination of the energy spectra of the gamma radiation.

However, on Leg 7 of the D/V *Glomar Challenger* the system provided data which permit some statements to be made concerning the general level of gamma radiation of the sediments penetrated.

This report summarizes and evaluates natural gamma radiation data collected on Leg 7, and attempts to interpret some of the findings.

METHODS

The natural gamma radiation of almost all sections recovered on Leg 7 of the D/V *Glomar Challenger* was measured by passing the unsplit core section through a natural gamma scanning system. The system used consists of (1) four shielded 3 by 3 inch scintillation detectors located 90 degrees apart in a plane normal to the length of the core section; (2) an incremented time step core transport mechanism set to advance a section through three inches per step each 1.25 minutes; (3) two dual input, single channel analyzers to accumulate total count rate; (4) a timing unit to regulate both core transport and counting times; (5) a digital to analog converter to supply the analog count rate to two strip recorders; and (6) a printer which yields a tabulation of total count. Details of the system are described by Evans and Lucia (1970) and by Maxwell *et al.* (1970).

The unit includes neither a pulse-height analyzer nor a multi-channel analyzer, but measures the total count through a fixed window. Gamma rays having an energy equal to or greater than 0.3 Mev are passed and counted.

The gamma ray scanning device aboard the *Glomar Challenger* has not been rigorously calibrated. However, in most cases, two controls were run before the natural gamma radiation was measured on each core. The first was an "air" standard wherein the counter was left running with nothing in the scanner for a series of 1.25 minute readings. The second was a "water" standard wherein a series of natural gamma radiation measurements were made of a section of plastic core liner filled with sea water.

An arithmetic mean of the measurements of the air and water controls was obtained for each series of tests. These means are listed next to the appropriate sections in Table 1 and are plotted for the appropriate sections as a function of depth on Figures 1 through 6. Their frequency distribution is shown on Figure 10. The means of the water control measurements range from 1379 to 1556 counts per 1.25 minutes; 88 per cent of the means are between 1450 and 1525 counts; and the median of these values is 1495. The mean air control measurements range from 1361 to 1616 counts per 1.25 minutes; 90 per cent of the controls are between 1400 and 1475, and the median of these values is 1445. The higher measurements for the water controls probably reflect radioactivity of the plastic liner and the seawater it contains.

When variations in the measurements of the controls are compared with the measurement of the gamma radiation of sections made immediately after the standards were run, no consistent correlation between background count and counts on the cores can be seen, even when the sediments show very low levels of radiation. Why there is no correlation is uncertain, but it may be that the cores provide more shielding against extraneous radiation in the laboratory entering into the access hole in the lead shielding of the system than does the open hole or even the water blank. The air controls reflect even less shielding effect than the water, and the wider range of mean values for the air controls reflects this. If these conditions prevail, the actual background count for sediment cores will be lower and less erratic than either the water or air controls.

On Leg 4 at Site 29 (Gealy and Gerard, 1970), *in-situ* gamma radiation was measured with a calibrated logging tool. When the values so obtained were

TABLE 1
Natural Gamma Radiation

Leg	Hole	Core	Section	Depth Below Sea Floor (Meters)	γ^a Gamma Radiation	Mean Water Control	Mean Air Control	ϕ Porosity Fraction	1-ϕ Solid Fraction	$\gamma/(1-\phi)$	CO_3 Weight Fraction	1-CO_3 Weight Fraction	$(1-\phi)(1-CO_3)$ Weight Fraction	$\gamma/(1-\phi)(1-CO_3)$
Site 61														
7	61.1	1	1	83.75	344	1379	1361	0.495	0.505	681	0	1.000	0.505	681
7	61.1	1	2	85.25	519	1379	1361	0.408	0.592	876	0	1.000	0.592	876
Site 62														
7	62	1	1	91.75	405		1429	0.604	0.396	1023	0.848	0.152	0.060	6729
7	62	1	1	93.25	341		1429	0.618	0.382	894	0.823	0.177	0.068	5050
7	62	1	3	94.75	341		1429	0.608	0.392	872	0.875	0.125	0.049	6973
7	62	1	4	96.25	301		1429	0.623	0.377	798	0.848	0.152	0.057	5250
7	62	1	5	97.75	350		1429	0.624	0.376	932	0.793	0.207	0.078	4504
7	62	1	6	99.25	390		1429	0.629	0.371	1052	0.856	0.144	0.053	7307
7	62	2	1	205.75	177	1509	1451	0.768	0.232	765	0.895	0.105	0.024	7231
7	62	2	2	207.25	228	1509	1451	0.584	0.416	549	0.896	0.104	0.043	5234
7	62	2	3	208.75	196	1509	1451	0.584	0.416	471	0.870	0.130	0.054	3621
7	62	2	4	210.25	205	1509	1451	0.585	0.415	494	0.895	0.105	0.044	4704
7	62	2	5	211.75	214	1509	1451	0.581	0.419	511	0.909	0.091	0.038	5610
7	62	2	6	213.25	222	1509	1451	0.582	0.418	533	0.938	0.062	0.026	8590
7	62	3	1	299.75	206	1462	1449	0.572	0.428	481	0.910	0.090	0.039	5350
7	62	3	2	301.25	182	1462	1449	0.586	0.414	440	0.970	0.030	0.012	14654
7	62	3	2	302.25	186	1462	1449	0.519	0.421	442	0.886	0.114	0.048	3878
7	62	3	4	304.25	198	1462	1449	0.576	0.424	466	0.908	0.092	0.039	5054
7	62	3	5	305.75	205	1462	1449	0.558	0.442	464	0.940	0.060	0.027	7740
7	62	3	6	307.25	215	1462	1449	0.581	0.419	513	0.883	0.117	0.049	4335
7	62	4	1	395.75	273	1487	1429	0.567	0.433	631	0.783	0.217	0.094	2910
7	62	4	2	397.25	296	1490	1393	0.496	0.304	587	0.857	0.143	0.072	4107
7	62	4	3	398.75	262	1490	1393	0.501	0.499	525	0.828	0.172	0.086	3052
7	62	4	4	400.25	249	1490	1393	0.599	0.401	620	0.810	0.190	0.076	3262

TABLE 1 – *Continued*

Leg	Hole	Core	Section	Depth Below Sea Floor (Meters)	γ[a] Gamma Radiation	Mean Water Control	Mean Air Control	ϕ Porosity Fraction	1-ϕ Solid Fraction	$\gamma/(1-\phi)$	CO_3 Weight Fraction	1-CO_3 Weight Fraction	(1-ϕ)(1-CO_3) Weight Fraction	$\gamma/(1-\phi)(1-CO_3)$
Site 62 – *Continued*														
7	62	4	5	401.75	206	1490	1393	0.522	0.478	556	0.835	0.165	0.079	3373
7	62	4	6	403.25	255	1490	1393	0.576	0.424	602	0.797	0.203	0.086	2957
7	62	5	2	492.25	112	1458	1387	0.503	0.497	226	0.891	0.109	0.054	2073
7	62	5	3	493.75	81	1458	1387	0.482	0.518	157	0.886	0.114	0.059	1373
7	62	5	4	495.25	120	1458	1387	0.449	0.551	217	0.927	0.073	0.040	2975
7	62.1	1	2	8.25	918	1505	1438	0.768	0.232	3959	0.621	0.379	0.088	10446
7	62.1	1	3	9.75	557	1505	1438	0.711	0.289	1927	0.565	0.435	0.126	4429
7	62.1	4	1	34.75	385	1486	1429	0.719	0.281	1368	0.722	0.278	0.078	4921
7	62.1	4	2	36.25	367	1486	1429	0.708	0.294	1250	0.710	0.290	0.085	4310
7	62.1	4	4	39.25	369	1486	1429	0.688	0.312	1184	0.798	0.202	0.063	5852
7	62.1	4	5	40.75	321	1486	1429	0.673	0.327	981	0.801	0.199	0.065	4931
7	62.1	4	6	42.25	343	1486	1429	0.676	0.324	1058	0.758	0.242	0.078	4372
7	62.1	6	1	54.75	360	1470	1411	0.715	0.285	1265	0.501	0.499	0.142	2535
7	62.1	6	2	56.25	347	1470	1411	0.712	0.288	1206	0.810	0.190	0.055	6346
7	62.1	6	3	57.75	346	1470	1411	0.709	0.291	1188	0.736	0.264	0.077	4501
7	62.1	6	4	59.25	345	1470	1411	0.700	0.300	1149	0.591	0.409	0.123	2809
7	62.1	6	5	60.75	359	1470	1411	0.696	0.304	1183	0.743	0.257	0.078	4604
7	62.1	6	6	62.25	314	1470	1411	0.665	0.335	938	0.760	0.240	0.080	3907
7	62.1	7	1	63.75	347	1514	1451	0.688	0.312	1113	0.675	0.325	0.101	3426
7	62.1	7	2	65.25	346	1502	1485	0.657	0.343	1007	0.630	0.350	0.120	2877
7	62.1	7	3	66.75	404	1502	1485	0.679	0.321	1258	0.743	0.257	0.082	4896
7	62.1	7	4	68.25	396	1502	1485	0.691	0.309	1280	0.618	0.382	0.118	3351
7	62.1	7	5	69.75	397	1502	1485	0.644	0.356	1115	0.883	0.117	0.042	9529
7	62.1	7	6	71.25	388	1502	1485	0.675	0.325	1195	0.770	0.230	0.075	5197
7	62.1	8	2	74.25	349	1507	1455	0.645	0.355	984	0.648	0.352	0.125	2794

TABLE 1 – *Continued*

Leg	Hole	Core	Section	Depth Below Sea Floor (Meters)	γ^a Gamma Radiation	Mean Water Control	Mean Air Control	ϕ Porosity Fraction	1-ϕ Solid Fraction	$\gamma/(1-\phi)$	CO_3 Weight Fraction	1-CO_3 Weight Fraction	$(1-\phi)(1-CO_3)$ Weight Fraction	$\gamma/(1-\phi)(1-CO_3)$
Site 62 – *Continued*														
7	62.1	8	3	75.75	371	1507	1455	0.655	0.345	1075	0.681	0.319	0.110	3371
7	62.1	8	4	77.25	397	1507	1455	0.642	0.358	1108	0.812	0.188	0.067	5897
7	62.1	8	5	78.75	448	1507	1455	0.651	0.349	1286	0.736	0.264	0.092	4870
7	62.1	8	6	80.25	385	1507	1455	0.644	0.356	1081	0.729	0.271	0.097	3988
7	62.1	9	2	83.25	408	1522	1454	0.659	0.341	1194	0.791	0.209	0.071	5715
7	62.1	9	4	86.25	409	1500	1443	0.663	0.337	1214	0.625	0.375	0.126	3236
7	62.1	9	3	84.75	398	1500	1443	0.636	0.364	1093	0.740	0.260	0.095	4205
7	62.1	10	1	92.75	355	1518	1449	0.673	0.327	1086	0.478	0.522	0.171	2080
7	62.1	10	2	94.25	362	1485	1438	0.688	0.312	1161	0.760	0.240	0.075	4838
7	62.1	10	3	95.75	508	1485	1438	0.673	0.327	1553	0.655	0.345	0.113	4500
7	62.1	10	4	97.25	427	1485	1438	0.674	0.326	1311	0.759	0.231	0.075	5675
7	62.1	10	5	98.75	489	1485	1438	0.665	0.335	1459	0.725	0.275	0.092	5304
7	62.1	10	6	100.25	413	1485	1438	0.638	0.362	1142	0.770	0.230	0.083	4955
7	62.1	11	1	101.75	387	1517	1438	0.629	0.371	1043	0.785	0.215	0.080	4852
7	62.1	11	2	103.25	364	1517	1417	0.653	0.347	1049	0.785	0.215	0.075	4877
7	62.1	11	3	104.75	388	1517	1417	0.640	0.360	1078	0.792	0.208	0.075	5183
7	62.1	11	4	106.25	393	1517	1417	0.639	0.361	1087	0.689	0.311	0.112	3495
7	62.1	11	5	107.75	455	1517	1417	0.644	0.356	1279	0.769	0.231	0.082	5539
7	62.1	11	6	109.25	357	1517	1417	0.648	0.352	1014	0.776	0.224	0.079	4526
7	62.1	12	1	110.75	361	1477	1486	0.645	0.355	1017	0.789	0.211	0.075	4819
7	62.1	12	2	112.25	324	1502	1432	0.638	0.362	895	0.836	0.164	0.059	5456
7	62.1	12	3	113.75	319	1502	1432	0.616	0.384	832	0.840	0.160	0.061	5197
7	62.1	12	4	115.25	339	1502	1432	0.604	0.396	855	0.835	0.165	0.065	5182
7	62.1	12	5	116.75	318	1502	1432	0.629	0.371	856	0.824	0.176	0.065	4856
7	62.1	12	6	118.25	348	1502	1432	0.609	0.391	890	0.862	0.138	0.054	6449

TABLE 1 – *Continued*

Leg	Hole	Core	Section	Depth Below Sea Floor (Meters)	γ^a Gamma Radiation	Mean Water Control	Mean Air Control	ϕ Porosity Fraction	1-ϕ Solid Fraction	$\gamma/(1-\phi)$	CO_3 Weight Fraction	1-CO_3 Weight Fraction	$(1-\phi)(1-CO_3)$ Weight Fraction	$\gamma/(1-\phi)(1-CO_3)$
Site 62 – *Continued*														
7	62.1	13	5	125.75	312	1493	1455	0.646	0.354	881	0.840	0.160	0.057	5504
7	62.1	14	1	129.75	274	1516	1449	0.651	0.349	786	0.859	0.141	0.049	5577
7	62.1	14	2	131.25	273	1490	1486	0.686	0.314	869	0.845	0.155	0.049	5604
7	62.1	14	3	132.75	274	1490	1486	0.643	0.357	766	0.866	0.134	0.048	5716
7	62.1	14	4	134.25	270	1490	1486	0.637	0.363	744	0.778	0.222	0.081	3351
7	62.1	14	5	135.75	265	1490	1486	0.684	0.336	789	0.856	0.144	0.048	5432
7	62.1	14	6	137.25	305	1490	1486	0.722	0.278	1095	0.843	0.157	0.044	6977
7	62.1	15	1	138.75	296	1505	1446	0.613	0.387	765	0.418	0.582	0.225	1315
7	62.1	15	2	140.25	288	1478	1439	0.623	0.377	765	0.856	0.144	0.054	5310
7	62.1	15	3	141.75	297	1478	1439	0.622	0.378	787	0.856	0.134	0.051	5875
7	62.1	15	4	143.25	336	1478	1439	0.621	0.379	885	0.601	0.399	0.151	2219
7	62.1	15	5	144.75	310	1478	1439	0.619	0.381	815	0.676	0.324	0.123	2517
7	62.1	15	6	146.25	318	1478	1439	0.613	0.387	820	0.829	0.171	0.066	4797
7	62.1	16	1	147.75	333	1520	1453	0.635	0.365	911	0.901	0.099	0.036	9204
7	62.1	16	2	149.25	302	1520	1453	0.627	0.373	809	0.885	0.115	0.043	7036
7	62.1	16	3	150.75	293	1520	1453	0.606	0.394	742	0.868	0.132	0.052	5624
7	62.1	16	4	152.25	314	1520	1453	0.598	0.402	781	0.836	0.164	0.066	4762
7	62.1	16	5	153.75	268	1520	1453	0.604	0.396	677	0.892	0.108	0.043	6269
7	62.1	16	6	155.25	275	1520	1453	0.584	0.416	660	0.807	0.193	0.080	3422
7	62.1	17	1	156.75	310	1520	1453	0.631	0.369	840	0.864	0.136	0.050	6174
7	62.1	17	2	158.25	314	1517	1409	0.604	0.396	792	0.864	0.136	0.054	5821
7	62.1	17	3	159.75	318	1491	1460	0.604	0.396	805	0.973	0.027	0.011	29815
7	62.1	17	4	161.25	318	1491	1460	0.596	0.404	788	0.897	0.103	0.042	7654
7	62.1	17	5	162.75	269	1491	1460	0.591	0.408	658	0.930	0.070	0.029	9393
7	62.1	17	6	164.25	352	1491	1460	0.586	0.414	850	0.832	0.168	0.069	5060

TABLE 1 – *Continued*

Leg	Hole	Core	Section	Depth Below Sea Floor (Meters)	γ[a] Gamma Radiation	Mean Water Control	Mean Air Control	ϕ Porosity Fraction	1-ϕ Solid Fraction	$\gamma/(1-\phi)$	CO_3 Weight Fraction	1-CO_3 Weight Fraction	$(1-\phi)(1-CO_3)$ Weight Fraction	$\gamma/(1-\phi)(1-CO_3)$
Site 62 – *Continued*														
7	62.1	18	1	165.75	269	1468	1421	0.556	0.444	606	0.830	0.120	0.053	5052
7	62.1	18	2	167.25	263	1496	1421	0.560	0.440	597	0.911	0.089	0.039	6711
7	62.1	18	3	168.75	288	1496	1425	0.589	0.411	702	0.940	0.060	0.025	11700
7	62.1	18	4	170.25	287	1496	1425	0.566	0.434	662	0.935	0.065	0.028	10132
7	62.1	18	5	171.75	227	1496	1425	0.578	0.422	538	0.879	0.121	0.051	4446
7	62.1	18	6	173.25	313	1496	1425	0.559	0.441	710	0.888	0.112	0.049	6339
7	62.1	19	1	174.75	280	1469	1473	0.619	0.381	736	0.917	0.083	0.032	8865
7	62.1	19	2	176.25	242	1492	1616	0.611	0.389	621	0.946	0.054	0.021	11507
7	62.1	19	3	177.75	283	1492	1616	0.555	0.445	637	0.960	0.040	0.018	15915
7	62.1	19	4	179.25	267	1492	1616	0.583	0.437	610	0.924	0.076	0.033	8026
7	62.1	19	5	180.75	272	1492	1616	0.596	0.404	672	0.920	0.080	0.032	8398
7	62.1	19	6	182.25	294	1492	1616	0.560	0.440	669	0.620	0.380	0.167	1762
7	62.1	20	1	186.75	155	1495	1452	0.590	0.410	621	0.908	0.092	0.038	6749
7	62.1	20	2	188.25	256	1495	1452	0.578	0.422	605	0.790	0.210	0.089	2882
7	62.1	20	3	189.75	253	1495	1452	0.574	0.426	594	0.931	0.069	0.029	8611
7	62.1	20	4	191.25	265	1495	1452	0.561	0.439	604	0.894	0.106	0.047	5694
7	62.1	20	5	192.75	236	1495	1452	0.573	0.427	552	0.930	0.070	0.030	7836
7	62.1	20	6	194.25	255	1495	1452	0.569	0.431	592	0.929	0.071	0.031	8339
7	62.1	21	1	195.75	213	1488	1443	0.587	0.413	514	0.888	0.112	0.046	4593
7	62.1	21	2	197.25	266	1506	1459	0.553	0.447	596	0.943	0.057	0.025	10452
7	62.1	21	3	198.75	255	1506	1459	0.550	0.450	567	0.894	0.106	0.048	5346
7	62.1	21	4	200.25	231	1506	1459	0.541	0.459	502	0.833	0.167	0.077	3008
7	62.1	21	5	201.75	243	1506	1459	0.540	0.460	527	0.934	0.066	0.030	7985
7	62.1	21	6	203.25	173	1506	1459	0.537	0.463	374	0.745	0.255	0.118	1465
7	62.1	22	1	207.75	223	1506	1459	0.583	0.437	510	0.922	0.078	0.034	6535

TABLE 1 – *Continued*

Leg	Hole	Core	Section	Depth Below Sea Floor (Meters)	γ[a] Gamma Radiation	Mean Water Control	Mean Air Control	ϕ Porosity Fraction	1-ϕ Solid Fraction	$\gamma/(1-\phi)$	CO_3 Weight Fraction	1-CO_3 Weight Fraction	$(1-\phi)(1-CO_3)$ Weight Fraction	$\gamma/(1-\phi)(1-CO_3)$
Site 62 – *Continued*														
7	62.1	22	2	209.25	229	1489	1463	0.560	0.440	520	0.926	0.074	0.033	7021
7	62.1	22	3	210.75	245	1489	1463	0.535	0.465	527	0.898	0.102	0.047	5263
7	62.1	22	4	212.25	224	1489	1463	0.552	0.448	500	0.905	0.095	0.043	5262
7	62.1	22	5	213.75	209	1489	1463	0.527	0.473	442	0.921	0.079	0.037	5594
7	62.1	22	6	215.25	230	1489	1463	0.574	0.426	540	0.914	0.086	0.037	6283
7	62.1	23	1	216.75	234	1497	1471	0.558	0.442	531	0.879	0.121	0.053	4384
7	62.1	23	2	218.25	233	1503	1429	0.545	0.455	513	0.752	0.248	0.113	2067
7	62.1	23	3	219.75	250	1503	1429	0.542	0.458	547	0.603	0.397	0.182	1377
7	62.1	23	4	221.25	244	1503	1429	0.539	0.461	530	0.892	0.108	0.050	4906
7	62.1	23	5	222.75	222	1503	1429	0.546	0.454	489	0.696	0.304	0.138	1608
7	62.1	23	6	224.25	228	1503	1429	0.532	0.468	488	0.911	0.089	0.042	5479
7	62.1	24	1	225.75	220	1496	1415	0.530	0.470	467	0.975	0.025	0.012	18690
7	62.1	24	2	227.25	205	1446	1428	0.567	0.433	474	0.940	0.060	0.026	7907
7	62.1	24	3	228.75	227	1446	1428	0.549	0.451	504	0.900	0.100	0.045	5042
7	62.1	24	4	230.25	243	1446	1428	0.549	0.451	538	0.905	0.095	0.043	5656
7	62.1	24	5	231.75	244	1446	1428	0.557	0.443	550	0.691	0.309	0.137	1730
7	62.1	24	6	233.25	225	1446	1428	0.548	0.452	499	0.860	0.140	0.063	3554
7	62.1	25	1	234.75	248	1530	1463	0.575	0.425	583	0.905	0.095	0.040	6136
7	62.1	25	2	236.25	229	1501	1426	0.752	0.248	923	0.871	0.129	0.032	7152
7	62.1	25	3	237.75	250	1501	1426	0.594	0.406	615	0.887	0.113	0.046	5444
7	62.1	25	4	239.25	254	1501	1426	0.574	0.426	595	0.853	0.147	0.063	4050
7	62.1	25	5	240.75	223	1501	1426	0.773	0.227	984	0.873	0.127	0.029	7746
7	62.1	26	1	245.75	251	1528	1468	0.569	0.431	583	0.764	0.236	0.102	2459
7	62.1	26	3	248.75	256	1509	1451	0.567	0.433	592	0.848	0.152	0.066	3892
7	62.1	26	4	250.25	231	1509	1451	0.561	0.439	526	0.843	0.157	0.069	3350

TABLE 1 – *Continued*

Leg	Hole	Core	Section	Depth Below Sea Floor (Meters)	γ^a Gamma Radiation	Mean Water Control	Mean Water Control	ϕ Porosity Fraction	$1-\phi$ Solid Fraction	$\gamma/(1-\phi)$	CO_3 Weight Fraction	$1-CO_3$ Weight Fraction	$(1-\phi)(1-CO_3)$ Weight Fraction	$\gamma/(1-\phi)(1-CO_3)$
Site 62 – *Continued*														
7	62.1	26	5	251.75	212	1509	1451	0.582	0.418	506	0.931	0.069	0.029	7330
7	62.1	26	6	253.25	211	1509	1451	0.605	0.395	532	0.853	0.147	0.058	3622
7	62.1	27	1	254.75	204	1507	1471	0.611	0.389	523	0.895	0.105	0.041	4935
7	62.1	27	2	256.25	216	1483	1445	0.588	0.412	525	0.860	0.140	0.058	3748
7	62.1	27	3	257.75	232	1483	1445	0.577	0.423	549	0.743	0.257	0.109	2135
7	62.1	27	4	259.25	206	1483	1445	0.554	0.446	462	0.880	0.120	0.054	3849
7	62.1	27	5	260.75	224	1483	1445	0.556	0.444	503	0.896	0.104	0.046	4839
7	62.1	28	1	263.75	210	1530	1450	0.608	0.392	535	0.859	0.141	0.055	3793
7	62.1	28	2	265.25	214	1512	1481	0.589	0.411	521	0.868	0.132	0.054	3948
7	62.1	28	3	266.75	222	1512	1481	0.567	0.433	512	0.817	0.183	0.079	2799
7	62.1	28	4	268.25	219	1512	1481	0.599	0.401	545	0.743	0.257	0.103	2119
7	62.1	28	5	269.75	203	1512	1481	0.616	0.384	529	0.804	0.196	0.075	2701
7	62.1	28	6	271.25	210	1512	1481	0.608	0.392	535	0.519	0.481	0.188	1113
7	62.1	29	1	271.75	217	1500	1463	0.603	0.397	547	0.920	0.080	0.032	6838
7	62.1	29	2	273.25	197	1470	1437	0.605	0.395	500	0.864	0.136	0.054	3677
7	62.1	29	3	274.75	219	1470	1437	0.593	0.407	538	0.845	0.155	0.063	3471
7	62.1	29	4	276.25	205	1470	1437	0.609	0.391	525	0.844	0.156	0.061	3363
7	62.1	29	5	277.75	193	1470	1437	0.595	0.405	476	0.864	0.136	0.055	3502
7	62.1	29	6	279.25	205	1470	1437	0.599	0.401	512	0.851	0.149	0.060	3435
7	62.1	30	1	281.75	215	1521	1458	0.578	0.422	509	0.875	0.125	0.053	4074
7	62.1	30	2	283.25	181	1481	1424	0.586	0.414	437	0.875	0.125	0.052	3494
7	62.1	30	3	284.75	217	1481	1424	0.567	0.433	500	0.876	0.124	0.054	4035
7	62.1	30	4	286.25	191	1481	1424	0.574	0.426	448	0.908	0.092	0.039	4867
7	62.1	30	5	287.75	200	1481	1424	0.576	0.424	471	0.891	0.109	0.046	4317
7	62.1	30	6	289.25	184	1481	1424	0.592	0.408	450	0.407	0.593	0.242	759

TABLE 1 – *Continued*

Leg	Hole	Core	Section	Depth Below Sea Floor (Meters)	γ[a] Gamma Radiation	Mean Water Control	Mean Air Control	ϕ Porosity Fraction	$1-\phi$ Solid Fraction	$\gamma/(1-\phi)$	CO_3 Weight Fraction	$1-CO_3$ Weight Fraction	$(1-\phi)(1-CO_3)$ Weight Fraction	$\gamma/(1-\phi)(1-CO_3)$
Site 62 – *Continued*														
7	62.1	31	1	291.75	207	1506	1472	0.558	0.442	469	0.876	0.124	0.055	3782
7	62.1	31	2	293.25	211	1507	1476	0.567	0.433	487	0.858	0.142	0.061	3432
7	62.1	31	3	294.75	203	1507	1476	0.551	0.449	452	0.870	0.130	0.058	3480
7	62.1	31	4	296.25	199	1507	1476	0.546	0.454	439	0.860	0.140	0.064	3132
7	62.1	31	5	297.75	177	1507	1476	0.599	0.401	441	0.881	0.119	0.048	3708
7	62.1	31	6	299.25	204	1507	1476	0.551	0.449	454	0.895	0.105	0.047	4326
7	62.1	32	1	301.75	201	1481	1437	0.584	0.416	484	0.893	0.107	0.045	4519
7	62.1	32	2	303.25	175	1494	1474	0.568	0.432	406	0.906	0.094	0.041	4319
7	62.1	32	3	304.75	213	1494	1474	0.576	0.424	502	0.930	0.070	0.030	7174
7	62.1	32	4	306.25	247	1494	1474	0.581	0.419	589	0.743	0.257	0.108	2290
7	62.1	32	5	307.75	210	1494	1474	0.581	0.419	502	0.893	0.107	0.045	4689
7	62.1	32	6	309.25	237	1494	1474	0.581	0.419	566	0.866	0.134	0.056	4223
7	62.1	33	2	312.25	210	1474	1432	0.569	0.431	489	0.836	0.164	0.071	2980
7	62.1	33	3	313.75	228	1556	1469	0.559	0.441	518	0.808	0.192	0.085	2699
7	62.1	34	1	320.75	296	1476	1455	0.579	0.421	704	0.813	0.187	0.079	3763
7	62.1	34	2	322.25	267	1490	1450	0.536	0.464	575	0.851	0.149	0.069	3859
7	62.1	34	3	323.75	316	1490	1450	0.545	0.455	695	0.776	0.224	0.102	3101
7	62.1	34	4	325.25	288	1490	1450	0.542	0.458	628	0.827	0.173	0.079	3630
7	62.1	34	5	326.75	293	1490	1450	0.519	0.481	609	0.836	0.144	0.069	4226
7	62.1	34	6	328.25	248	1490	1450	0.520	0.480	516	0.869	0.131	0.063	3937
7	62.1	35	1	327.75	244	1505	1460	0.592	0.408	600	0.775	0.225	0.092	2665
7	62.1	35	2	329.25	214	1489	1463	0.591	0.409	523	0.833	0.167	0.068	3133
7	62.1	35	3	330.75	253	1489	1463	0.575	0.425	594	0.846	0.154	0.065	3858
7	62.1	35	4	332.25	266	1489	1463	0.572	0.428	620	0.836	0.164	0.070	3735
7	62.1	35	5	333.75	240	1489	1463	0.583	0.417	577	0.800	0.200	0.083	2885

TABLE 1 – *Continued*

Leg	Hole	Core	Section	Depth Below Sea Floor (Meters)	γ^a Gamma Radiation	Mean Water Control	Mean Air Control	ϕ Porosity Fraction	1-ϕ Solid Fraction	$\gamma/(1-\phi)$	CO_3 Weight Fraction	1-CO_3 Weight Fraction	$(1-\phi)(1-CO_3)$ Weight Fraction	$\gamma/(1-\phi)(1-CO_3)$
Site 62 – *Continued*														
7	62.1	35	6	335.25	253	1489	1463	0.570	0.430	588	0.846	0.154	0.066	3817
7	62.1	36	2	338.25	219	1505	1432	0.592	0.408	538	0.848	0.152	0.062	3541
7	62.1	36	3	339.75	232	1505	1432	0.571	0.429	541	0.833	0.167	0.072	3237
7	62.1	36	4	341.25	241	1505	1432	0.537	0.463	520	0.883	0.117	0.054	4448
7	62.1	36	5	342.75	263	1505	1432	0.505	0.435	604	0.855	0.145	0.063	4165
7	62.1	37	2	346.25	250	1498	1442	0.566	0.434	576	0.836	0.164	0.071	3513
Site 63														
7	63	1	1	.75	1582	1455	1424	0.767	0.233	6776	0.036	0.964	0.225	7029
7	63	1	2	2.25	906	1455	1424	0.770	0.230	3938	0.080	0.920	0.212	4230
7	63	1	3	3.75	721	1455	1424	0.748	0.252	2864	0.106	0.894	0.225	3203
7	63	1	4	5.25	614	1455	1424	0.792	0.208	2952	0.120	0.880	0.183	3354
7	63	2	2	63.25	298	1483	1417	0.642	0.358	832	0.670	0.330	0.118	2522
7	63	2	3	64.75	216	1483	1417	0.608	0.392	549	0.810	0.190	0.075	2891
7	63	2	4	66.25	266	1483	1417	0.642	0.358	744	0.796	0.204	0.073	3646
7	63	2	5	67.75	260	1483	1417	0.614	0.386	675	0.810	0.190	0.073	3552
7	63	2	6	69.25	268	1483	1417	0.599	0.401	668	0.610	0.390	0.156	1713
7	63	3	2	139.25	258	1477	1437	0.589	0.411	628	0.640	0.360	0.148	1744
7	63	3	3	140.75	262	1477	1437	0.581	0.419	627	0.791	0.209	0.088	2998
7	63	3	4	142.25	323	1477	1437	0.593	0.407	793	0.566	0.434	0.177	1827
7	63	4	1	230.75	193	1493	1450	0.543	0.457	422	0.764	0.236	0.108	1787
7	63	4	2	232.25	194	1493	1450	0.494	0.506	383	0.778	0.222	0.112	1724
7	63	5	2	354.25	181	1472	1439	0.475	0.525	344	0.806	0.194	0.102	1773
7	63	6	2	458.75	172	1546	1431	0.457	0.543	316	0.886	0.114	0.062	2772
7	63	6	2	460.25	170	1546	1431	0.479	0.521	326	0.906	0.094	0.049	3470

TABLE 1 – *Continued*

Leg	Hole	Core	Section	Depth Below Sea Floor (Meters)	γ[a] Gamma Radiation	Mean Water Control	Mean Air Control	ϕ Porosity Fraction	1-ϕ Solid Fraction	$\gamma/(1-\phi)$	CO_3 Weight Fraction	1-CO_3 Weight Fraction	$(1-\phi)(1-CO_3)$ Weight Fraction	$\gamma/(1-\phi)(1-CO_3)$
Site 63 – *Continued*														
7	63	6	3	461.75	181	1546	1431	0.446	0.554	327	0.900	0.100	0.055	3272
7	63	6	4	463.25	176	1546	1431	0.453	0.547	322	0.941	0.059	0.032	5449
7	63	6	5	464.75	193	1546	1431	0.436	0.564	342	0.900	0.100	0.056	3415
7	63	6	6	466.25	149	1546	1431	0.445	0.555	269	0.978	0.022	0.012	12238
7	63	7	1	534.75	126	1508	1431	0.440	0.560	225	0.872	0.128	0.072	1757
7	63	7	2	536.25	127	1508	1431	0.442	0.558	228	0.892	0.108	0.060	2113
7	63	7	3	537.75	146	1508	1431	0.417	0.583	251	0.863	0.137	0.080	1830
7	63	7	4	539.25	129	1508	1431	0.413	0.587	220	0.875	0.125	0.073	1759
7	63	7	5	540.75	132	1508	1431	0.399	0.601	220	0.850	0.120	0.072	1837
7	63	7	6	542.25	125	1508	1431	0.393	0.607	206	0.940	0.060	0.036	3433
7	63	8	2	545.25	135	1488	1414	0.438	0.562	239	0.891	0.109	0.061	2197
7	63	8	3	546.75	137	1488	1414	0.424	0.576	238	0.850	0.150	0.086	1537
7	63	9	1	553.75	124	1463	1450	0.388	0.612	202	0.913	0.087	0.053	2324
7	63	9	2	555.25	139	1463	1450	0.385	0.615	225	0.916	0.084	0.052	2631
7	63	9	3	556.75	126	1463	1450	0.359	0.641	196	0.918	0.082	0.053	2395
7	63	9	4	558.25	151	1463	1450	0.353	0.647	233	0.891	0.109	0.071	2142
7	63.1	1	1	3.75	566	1452	1420	0.819	0.181	3126	0.227	0.773	0.140	4043
7	63.1	1	2	5.25	637	1452	1420	0.812	0.188	3396	0.122	0.878	0.165	3868
6	63.1	1	3	6.75	568	1452	1420	0.815	0.185	3065	0.215	0.785	0.146	3905
7	63.1	1	4	8.25	515	1452	1420	0.862	0.138	3730	0.110	0.890	0.123	4191
7	63.1	3	1	22.75	446	1448	1450	0.795	0.205	2176	0.305	0.695	0.142	3131
7	63.1	3	2	24.25	707	1448	1450	0.776	0.224	3156	0.297	0.703	0.157	4490
7	63.1	5	1	101.75	222	1496	1426	0.691	0.309	718	0.624	0.376	0.116	1909
7	63.1	5	2	103.25	313	1496	1426	0.652	0.348	899	0.630	0.370	0.129	2430
7	63.1	5	3	104.75	284	1496	1426	0.647	0.353	806	0.712	0.288	0.102	2798

TABLE 1 – *Continued*

Leg	Hole	Core	Section	Depth Below Sea Floor (Meters)	γ^a Gamma Radiation	Mean Water Control	Mean Air Control	ϕ Porosity Fraction	1-ϕ Solid Fraction	$\gamma/(1-\phi)$	CO_3 Weight Fraction	1-CO_3 Weight Fraction	$(1-\phi)(1-CO_3)$ Weight Fraction	$\gamma/(1-\phi)(1-CO_3)$
Site 63 – *Continued*														
7	63.1	5	4	106.25	323	1496	1426	0.676	0.324	996	0.453	0.547	0.177	1821
7	63.1	6	1	101.75	286	1473	1436	0.718	0.282	1013	0.532	0.468	0.132	2165
7	63.1	6	2	112.25	429	1473	1436	0.707	0.293	1462	0.364	0.636	0.187	2298
7	63.1	6	3	113.75	379	1473	1436	0.703	0.297	1275	0.455	0.545	0.162	2340
7	63.1	6	4	115.25	402	1473	1436	0.693	0.307	1309	0.533	0.467	0.143	2803
7	63.1	6	5	116.75	403	1473	1436	0.674	0.326	1234	0.445	0.555	0.181	2224
7	63.1	6	6	118.25	362	1473	1436	0.844	0.356	1017	0.548	0.452	0.161	2249
7	63.1	7	2	121.25	336	1467	1429	0.703	0.297	1131	0.710	0.290	0.086	3902
7	63.1	7	3	122.75	364	1467	1429	0.699	0.301	1208	0.565	0.435	0.131	2777
7	63.1	7	4	124.25	385	1467	1429	0.700	0.300	1283	0.449	0.551	0.165	2328
7	63.1	8	3	132.75	257	1483	1446	0.896	0.104	2477	0.616	0.384	0.040	6449
7	63.1	8	4	134.25	293	1483	1446	0.792	0.208	1409	0.628	0.372	0.077	3788
7	63.1	8	5	135.75	316	1483	1446	0.768	0.232	1361	0.593	0.407	0.095	3343
7	63.1	9	1	138.75	277	1479	1431	0.848	0.352	785	0.736	0.264	0.093	2974
7	63.1	9	2	140.25	299	1479	1431	0.614	0.386	775	0.686	0.314	0.121	2468
7	63.1	9	3	141.75	317	1479	1431	0.621	0.379	837	0.776	0.224	0.085	3738
7	63.1	9	4	143.25	236	1479	1431	0.569	0.431	547	0.713	0.287	0.124	1905
7	63.1	9	5	144.75	281	1479	1431	0.601	0.399	705	0.635	0.365	0.146	1930
7	63.1	9	6	146.25	244	1479	1431	0.583	0.417	583	0.811	0.189	0.079	3087
7	63.1	10	1	148.75	281	1475	1422	0.596	0.404	695	0.704	0.296	0.120	2348
7	63.1	10	2	150.25	257	1475	1422	0.586	0.414	621	0.533	0.467	0.193	1329
7	63.1	10	3	151.75	317	1475	1422	0.617	0.383	827	0.717	0.283	0.108	2924
7	63.1	10	4	153.25	251	1475	1422	0.570	0.430	583	0.652	0.348	0.150	1676
7	63.1	10	5	154.75	249	1475	1422	0.566	0.434	573	0.796	0.204	0.088	2808
7	63.1	11	1	155.75	262	1477	1424	0.596	0.404	649	0.821	0.179	0.072	3624

TABLE 1 – *Continued*

Leg	Hole	Core	Section	Depth Below Sea Floor (Meters)	γ^a Gamma Radiation	Mean Water Control	Mean Air Control	ϕ Porosity Fraction	1-ϕ Solid Fraction	$\gamma/(1-\phi)$	CO_3 Weight Fraction	1-CO_3 Weight Fraction	$(1-\phi)(1-CO_3)$ Weight Fraction	$\gamma/(1-\phi)(1-CO_3)$
Site 63 – *Continued*														
7	63.1	11	2	157.25	287	1477	1424	0.625	0.375	763	0.656	0.344	0.129	2219
7	63.1	11	3	158.75	247	1477	1424	0.582	0.418	591	0.706	0.294	0.123	2011
7	63.1	11	4	160.25	214	1477	1424	0.563	0.437	490	0.780	0.220	0.096	2226
7	63.1	11	5	161.75	235	1477	1424	0.561	0.439	536	0.826	0.174	0.076	3080
7	63.1	11	6	163.25	267	1477	1424	0.544	0.456	584	0.706	0.294	0.134	1987
7	63.1	12	2	167.25	243	1515	1459	0.541	0.459	530	0.821	0.179	0.082	2960
7	63.1	13	1	174.75	235	1484	1428	0.572	0.428	549	0.765	0.235	0.100	2335
7	63.1	13	2	176.25	288	1484	1428	0.609	0.391	737	0.739	0.261	0.102	2823
7	63.1	13	3	177.75	275	1484	1428	0.557	0.443	621	0.780	0.220	0.098	2822
7	63.1	13	4	179.25	335	1484	1428	0.633	0.367	915	0.608	0.392	0.144	2333
7	63.1	13	5	180.75	232	1484	1428	0.574	0.426	544	0.723	0.277	0.118	1966
7	63.1	13	6	182.25	357	1484	1428	0.647	0.353	1012	0.463	0.537	0.189	1884
7	63.1	14	1	184.75	275	1549	1437	0.608	0.392	701	0.680	0.320	0.125	2192
7	63.1	14	2	186.25	247	1549	1437	0.554	0.446	534	0.803	0.197	0.088	2812
7	63.1	14	3	187.75	301	1549	1437	0.586	0.414	726	0.738	0.262	0.108	2771
7	63.1	14	4	189.25	241	1549	1437	0.570	0.430	561	0.581	0.419	0.180	1339
7	63.1	14	5	190.75	213	1549	1437	0.545	0.455	469	0.832	0.168	0.076	2793
7	63.2	1	3	14.75	531	1505	1437	0.794	0.206	2582	0.269	0.731	0.150	3532
7	63.2	1	4	16.25	586	1505	1437	0.823	0.177	3313	0.178	0.822	0.145	4030
7	63.2	2	1	20.75	526	1499	1461	0.801	0.199	2647	0.059	0.941	0.187	2813
7	63.2	2	2	22.25	531	1499	1461	0.825	0.175	3040	0.278	0.722	0.126	4210
7	63.2	2	3	23.75	543	1499	1461	0.838	0.162	3346	0.173	0.827	0.134	4046
7	63.2	2	4	25.25	522	1499	1461	0.839	0.161	3234	0.211	0.789	0.127	4099
7	63.2	2	6	28.25	498	1499	1461	0.884	0.116	4279	0.170	0.830	0.097	5155
7	63.2	3	1	30.75	536	1518	1452	0.805	0.195	2745	0.170	0.830	0.162	3307

TABLE 1 – *Continued*

Leg	Hole	Core	Section	Depth Below Sea Floor (Meters)	γ[a] Gamma Radiation	Mean Water Control	Mean Air Control	ϕ Porosity Fraction	1-ϕ Solid Fraction	$\gamma/(1-\phi)$	CO_3 Weight Fraction	1-CO_3 Weight Fraction	$(1-\phi)(1-CO_3)$ Weight Fraction	$\gamma/(1-\phi)(1-CO_3)$
Site 63 – *Continued*														
7	63.2	3	2	32.25	515	1518	1452	0.783	0.217	2372	0.141	0.859	0.186	2762
7	63.2	3	3	33.75	449	1518	1452	0.742	0.258	1742	0.522	0.478	0.123	3644
7	63.2	3	4	35.35	381	1518	1452	0.687	0.313	1216	0.542	0.458	0.143	2656
Site 64														
7	64	1	2	2.75	649	1503	1448	0.723	0.217	2339	0.813	0.187	0.052	12509
7	64	1	3	3.75	552	1503	1448	0.719	0.281	1962	0.806	0.194	0.055	10114
7	64	1	4	5.25	395	1503	1448	0.713	0.287	1378	0.778	0.222	0.064	6205
7	64	1	5	6.75	383	1503	1448	0.715	0.285	1342	0.826	0.174	0.050	7710
7	64	1	6	8.25	380	1503	1448	0.719	0.281	1352	0.821	0.179	0.050	7553
7	64	2	1	99.75	263	1504	1465	0.655	0.345	763	0.866	0.134	0.046	5696
7	64	2	2	101.25	224	1504	1465	0.660	0.340	660	0.885	0.115	0.039	5741
7	64	2	3	102.75	206	1504	1465	0.662	0.338	610	0.886	0.114	0.039	5353
7	64	2	6	107.25	228	1504	1465	0.619	0.381	598	0.910	0.090	0.034	6642
7	64	3	1	202.75	173	1501	1422	0.606	0.394	438	0.927	0.073	0.029	6001
7	64	3	2	204.25	139	1501	1422	0.590	0.410	340	0.955	0.045	0.018	7563
7	64	3	3	205.75	170	1501	1422	0.588	0.412	413	0.861	0.139	0.057	2969
7	64	3	4	207.25	194	1501	1422	0.608	0.392	494	0.931	0.069	0.027	7159
7	64	3	5	208.75	188	1501	1422	0.595	0.405	464	0.916	0.084	0.034	5522
7	64	3	6	210.25	172	1501	1422	0.597	0.403	426	0.876	0.124	0.050	3438
7	64	4	1	304.75	157	1489	1435	0.621	0.379	413	0.890	0.110	0.042	3757
7	64	4	2	306.25	142	1489	1435	0.615	0.385	369	0.883	0.117	0.045	3151
7	64	4	3	307.75	165	1489	1435	0.590	0.410	402	0.846	0.154	0.063	2607
7	64	4	4	309.25	139	1489	1435	0.594	0.406	343	0.710	0.290	0.118	1132
7	64	4	5	310.75	139	1489	1435	0.592	0.408	341	0.870	0.130	0.053	2622

TABLE 1 – *Continued*

Leg	Hole	Core	Section	Depth Below Sea Floor (Meters)	γ^a Gamma Radiation	Mean Water Control	Mean Air Control	ϕ Porosity Fraction	$1-\phi$ Solid Fraction	$\gamma/(1-\phi)$	CO_3 Weight Fraction	$1-CO_3$ Weight Fraction	$(1-\phi)(1-CO_3)$ Weight Fraction	$\gamma/(1-\phi)(1-CO_3)$
Site 64 – *Continued*														
7	64	4	6	312.25	177	1489	1435	0.585	0.415	427	0.910	0.090	0.037	4739
7	64	5	1	409.75	111	1489	1445	0.572	0.428	260	0.905	0.095	0.041	2737
7	64	5	2	411.25	150	1489	1445	0.591	0.409	367	0.863	0.137	0.056	2632
7	64	5	4	414.25	148	1489	1445	0.571	0.429	344	0.883	0.117	0.050	2944
7	64	5	5	415.75	169	1489	1445	0.554	0.446	378	0.836	0.164	0.073	2305
7	64	6	1	505.75	122	1467	1431	0.544	0.456	267	0.456	0.544	0.248	491
7	64	7	1	610.75	110	1438	1430	0.605	0.395	278	0.847	0.153	0.060	1818
7	64	7	3	613.75	130	1438	1430	0.562	0.438	297	0.869	0.131	0.057	2265
7	64	7	4	615.25	118	1438	1430	0.548	0.452	261	0.886	0.114	0.051	2290
7	64	7	6	618.25	104	1438	1430	0.586	0.414	250	0.910	0.090	0.037	2780
7	64	7	5	616.75	132	1438	1430	0.575	0.425	310	0.894	0.106	0.045	2923
7	64	8	2	707.25	126	1469	1422	0.471	0.529	237	0.859	0.141	0.075	1682
7	64	8	3	708.75	152	1469	1422	0.469	0.531	287	0.861	0.139	0.074	2064
7	64	10	1	848.75	192	1504	1410	0.500	0.500	385	0.879	0.121	0.060	3183
7	64	10	2	850.25	149	1504	1410	0.452	0.548	272	0.845	0.155	0.085	1752
7	64.1	1	1	433.75	116	1512	1445	0.546	0.454	255	0.907	0.093	0.042	2737
7	64.1	1	2	435.25	149	1512	1445	0.550	0.450	332	0.797	0.203	0.091	1634
7	64.1	1	3	436.75	147	1512	1445	0.559	0.441	333	0.693	0.307	0.135	1085
7	64.1	1	4	438.25	157	1512	1445	0.551	0.449	351	0.901	0.099	0.044	3541
7	64.1	1	5	439.75	128	1512	1445	0.532	0.468	273	0.908	0.092	0.043	2970
7	64.1	1	6	441.25	157	1512	1445	0.566	0.434	362	0.854	0.136	0.059	2663
7	64.1	2	1	442.75	163	1522	1459	0.587	0.413	395	0.836	0.164	0.068	2408
7	64.1	2	2	444.25	159	1522	1459	0.574	0.426	372	0.850	0.150	0.064	2482
7	64.1	2	3	445.75	140	1522	1459	0.547	0.453	309	0.820	0.180	0.081	1720
7	64.1	2	4	447.25	168	1522	1459	0.531	0.469	357	0.886	0.114	0.054	3133

TABLE 1 – *Continued*

Leg	Hole	Core	Section	Depth Below Sea Floor (Meters)	γ^a Gamma Radiation	Mean Water Control	Mean Air Control	ϕ Porosity Fraction	1-ϕ Solid Fraction	$\gamma/(1-\phi)$	CO_3 Weight Fraction	1-CO_3 Weight Fraction	$(1-\phi)(1-CO_3)$ Weight Fraction	$\gamma/(1-\phi)(1-CO_3)$
Site 64 – *Continued*														
7	64.1	2	5	448.75	134	1522	1459	0.544	0.456	294	0.886	0.114	0.052	2577
7	64.1	2	6	450.25	151	1522	1459	0.532	0.468	323	0.915	0.085	0.040	3802
7	64.1	3	1	451.75	159	1475	1435	0.531	0.469	339	0.893	0.107	0.050	3171
7	64.1	3	2	453.25	153	1475	1435	0.535	0.445	343	0.874	0.126	0.056	2723
7	64.1	3	3	454.75	121	1475	1435	0.542	0.458	265	0.901	0.099	0.045	2674
7	64.1	3	4	456.25	121	1475	1435	0.536	0.464	261	0.896	0.104	0.048	2509
7	64.1	3	5	457.75	142	1475	1435	0.556	0.444	320	0.929	0.071	0.032	4504
7	64.1	3	6	459.25	144	1475	1435	0.555	0.445	323	0.908	0.092	0.041	3513
7	64.1	4	1	461.75	157	1475	1450	0.568	0.432	363	0.866	0.134	0.058	2711
7	64.1	4	2	463.25	132	1475	1450	0.562	0.438	302	0.903	0.097	0.042	3111
7	64.1	4	4	466.25	161	1475	1450	0.566	0.434	370	0.865	0.135	0.059	2741
7	64.1	4	5	467.75	153	1475	1450	0.540	0.460	334	0.840	0.160	0.074	2085
7	64.1	4	6	469.25	157	1475	1450	0.528	0.472	333	0.875	0.125	0.059	2663
7	64.1	5	1	470.75	134	1494	1483	0.579	0.421	319	0.828	0.172	0.072	1856
7	64.1	5	2	472.25	163	1494	1483	0.556	0.444	366	0.850	0.150	0.067	2442
7	64.1	5	3	473.75	149	1494	1483	0.540	0.460	324	0.858	0.142	0.065	2233
7	64.1	5	4	475.25	153	1494	1483	0.523	0.477	320	0.902	0.098	0.047	3263
7	64.1	5	5	476.75	143	1494	1483	0.509	0.491	291	0.923	0.077	0.038	3779
7	64.1	5	6	478.25	144	1494	1483	0.523	0.476	303	0.886	0.114	0.054	2656
7	64.1	6	1	565.75	158	1502	1436	0.512	0.488	323	0.886	0.114	0.056	2837
7	64.1	6	2	567.25	137	1502	1436	0.529	0.471	290	0.875	0.125	0.059	2321
7	64.1	6	3	568.75	152	1502	1436	0.526	0.474	320	0.871	0.129	0.061	2432
7	64.1	6	4	570.25	110	1502	1436	0.521	0.479	229	0.916	0.084	0.040	2723
7	64.1	7	1	661.75	148	1507	1480	0.557	0.443	335	0.858	0.142	0.063	2356
7	64.1	7	2	663.25	154	1507	1480	0.516	0.484	318	0.810	0.190	0.092	1672

TABLE 1 – *Continued*

Leg	Hole	Core	Section	Depth Below Sea Floor (Meters)	γ[a] Gamma Radiation	Mean Water Control	Mean Air Control	ϕ Porosity Fraction	1-ϕ Solid Fraction	$\gamma/(1-\phi)$	CO_3 Weight Fraction	1-CO_3 Weight Fraction	$(1-\phi)(1-CO_3)$ Weight Fraction	$\gamma/(1-\phi)(1-CO_3)$
Site 64 – *Continued*														
7	64.1	7	3	664.75	161	1507	1480	0.515	0.485	333	0.843	0.157	0.076	2120
7	64.1	7	4	666.25	147	1507	1480	0.536	0.464	316	0.908	0.092	0.043	3433
7	64.1	8	2	748.25	168	1455	1439	0.487	0.513	326	0.893	0.107	0.055	3050
7	64.1	9	1	911.75	140	1500	1477	0.511	0.489	286	0.871	0.129	0.063	2218
7	64.1	9	2	913.25	113	1500	1477	0.515	0.485	234	0.920	0.080	0.039	2921
7	64.1	9	3	914.75	90	1500	1477	0.490	0.510	176	0.921	0.079	0.040	2231
7	64.1	10	1	969.75	109	1443	1437	0.517	0.483	227	0.826	0.174	0.084	1302
7	64.1	10	2	971.25	145	1443	1437	0.494	0.506	286	0.840	0.160	0.081	1788
Site 65														
7	65	2	1	10.75	322	1488	1440	0.915	0.085	3793	0	1.000	0.085	3793
7	65	2	2	12.25	339	1488	1440	0.912	0.088	3869	0.003	0.997	0.087	3881
7	65	2	3	13.75	341	1488	1440	0.909	0.091	3731	0.016	0.984	0.090	3792
7	65	2	4	15.25	333	1488	1440	0.916	0.084	3947	0.004	0.996	0.084	3963
7	65	2	5	16.75	302	1488	1440	0.911	0.089	3396	0.006	0.994	0.088	3416
7	65	3	1	19.75	326	1509	1435	0.907	0.093	3524	0.004	0.996	0.092	3538
7	65	3	2	21.25	312	1509	1435	0.912	0.088	3538	0.007	0.993	0.088	3563
7	65	3	3	22.75	369	1509	1435	0.912	0.088	4176	0.007	0.993	0.088	4205
7	65	3	4	24.25	343	1509	1435	0.900	0.100	3419	0.005	0.995	0.100	3436
7	65	3	5	25.75	369	1509	1435	0.901	0.099	3725	0.007	0.993	0.098	3751
7	65	5	2	39.25	342	1482	1454	0.898	0.102	3354	0.004	0.996	0.102	3368
7	65	5	4	42.25	299	1482	1454	0.894	0.106	2833	0.002	0.998	0.105	2839
7	65	5	5	43.75	309	1482	1454	0.908	0.092	3344	0.016	0.984	0.091	3398
7	65	5	6	45.25	283	1482	1454	0.922	0.078	3624	0.011	0.989	0.077	3665
7	65	6	2	48.25	243	1485	1456	0.899	0.101	2397	0.010	0.990	0.100	2421

TABLE 1 – *Continued*

Leg	Hole	Core	Section	Depth Below Sea Floor (Meters)	γ^a Gamma Radiation	Mean Water Control	Mean Air Control	ϕ Porosity Fraction	1-ϕ Solid Fraction	$\gamma/(1-\phi)$	CO_3 Weight Fraction	1-CO_3 Weight Fraction	(1-ϕ)(1-CO_3) Weight Fraction	$\gamma/(1-\phi)(1-CO_3)$
Site 65 – *Continued*														
7	65	7	2	57.25	348	1456	1411	0.891	0.109	3189	0.006	0.994	0.108	3208
7	65	7	3	58.75	353	1456	1411	0.884	0.116	3028	0.010	0.990	0.115	3058
7	65	7	4	60.25	370	1456	1411	0.903	0.097	3804	0.005	0.995	0.097	3823
7	65	7	5	61.75	350	1456	1411	0.911	0.089	3927	0.004	0.996	0.089	3942
7	65	8	1	64.75	324	1446	1445	0.872	0.128	2526	0.008	0.992	0.127	2546
7	65	8	2	66.25	331	1446	1445	0.869	0.131	2528	0.004	0.996	0.130	2538
7	65	8	3	67.75	302	1446	1445	0.847	0.153	1970	0.030	0.970	0.149	2031
7	65	8	4	69.25	322	1446	1445	0.884	0.116	2783	0.006	0.994	0.115	2800
7	65	8	5	70.75	305	1446	1445	0.855	0.145	2107	0.006	0.994	0.144	2120
7	65	8	6	72.25	332	1446	1445	0.864	0.136	2437	0.049	0.951	0.130	2562
7	65	9	1	74.75	315	1481	1490	0.843	0.157	2015	0.003	0.997	0.156	2021
7	65	9	2	76.25	310	1481	1490	0.850	0.150	2072	0.015	0.985	0.147	2103
7	65	9	3	77.75	246	1481	1490	0.845	0.155	1589	0.006	0.994	0.154	1599
7	65	9	5	80.75	283	1481	1490	0.353	0.147	1925	0.003	0.997	0.147	1930
7	65	10	1	83.75	213	1480	1443	0.359	0.141	1508	0.012	0.988	0.139	1526
7	65	10	3	86.75	271	1480	1443	0.845	0.155	1750	0.018	0.982	0.152	1782
7	65	10	4	88.25	263	1480	1443	0.847	0.153	1715	0	1.000	0.153	1715
7	65	11	2	94.25	254	1501	1433	0.890	0.110	2299	0.010	0.990	0.109	2323
7	65	11	3	95.75	266	1501	1433	0.887	0.113	2348	0.003	0.997	0.113	2355
7	65	11	4	97.25	274	1501	1433	0.897	0.103	2652	0.004	0.996	0.103	2663
7	65	11	5	98.75	280	1501	1433	0.913	0.087	3235	0.007	0.993	0.086	3258
7	65	11	6	100.25	266	1501	1433	0.923	0.077	3478	0	1.000	0.077	3478
7	65	12	1	101.75	293	1483	1460	0.937	0.063	4673	0.015	0.985	0.062	4744
7	65	12	2	103.25	318	1483	1460	0.892	0.108	2945	0.003	0.997	0.108	2954
7	65	12	3	104.75	293	1483	1460	0.890	0.110	2658	0.003	0.997	0.110	2666

TABLE 1 – *Continued*

Leg	Hole	Core	Section	Depth Below Sea Floor (Meters)	γ^a Gamma Radiation	Mean Water Control	Mean Air Control	ϕ Porosity Fraction	1-ϕ Solid Fraction	$\gamma/(1-\phi)$	CO_3 Weight Fraction	1-CO_3 Weight Fraction	$(1-\phi)(1-CO_3)$ Weight Fraction	$\gamma/(1-\phi)(1-CO_3)$
Site 65 – *Continued*														
7	65	12	4	106.25	503	1483	1460	0.828	0.172	2921	0.006	0.992	0.171	2944
7	65	12	5	107.75	288	1483	1460	0.878	0.122	2365	0.005	0.995	0.121	2377
7	65	12	6	109.25	270	1483	1460	0.891	0.109	2470	0.004	0.996	0.109	2430
7	65	13	1	110.75	243	1526	1459	0.920	0.080	3028	0.003	0.997	0.080	3038
7	65	13	2	112.25	241	1526	1459	0.912	0.088	2733	0	1.000	0.088	2733
7	65	13	3	113.75	260	1526	1459	0.888	0.112	2324	0	1.000	0.112	2324
7	65	13	4	115.25	270	1526	1459	0.889	0.111	2427	0.006	0.994	0.110	2442
7	65	13	5	116.75	277	1526	1459	0.884	0.116	2396	0.004	0.996	0.115	2406
7	65	13	6	118.25	260	1526	1459	0.877	0.123	2110	0.007	0.993	0.122	2125
7	65	14	1	119.75	262	1478	1443	0.885	0.115	2271	0.006	0.994	0.115	2285
7	65	14	2	121.25	266	1478	1443	0.860	0.140	1902	0.003	0.997	0.140	1908
7	65	14	3	122.75	293	1478	1443	0.806	0.194	1510	0.015	0.985	0.191	1533
7	65	14	4	124.25	296	1478	1443	0.769	0.231	1282	0.005	0.995	0.230	1238
7	65	14	5	125.75	273	1478	1443	0.742	0.258	1061	0.336	0.664	0.171	1598
7	65	14	6	127.25	269	1478	1443	0.681	0.319	842	0.372	0.628	0.200	1341
7	65	16	2	139.25	254	1491	1434	0.796	0.204	1241	0.141	0.859	0.175	1445
7	65	16	3	140.75	339	1491	1434	0.773	0.227	1491	0.145	0.855	0.194	1744
7	65	16	4	142.25	274	1491	1434	0.827	0.173	1586	0.027	0.973	0.168	1630
7	65	16	5	143.75	265	1491	1434	0.852	0.148	1795	0.040	0.960	0.142	1869
7	65	16	6	145.25	217	1491	1434	0.842	0.158	1370	0.013	0.987	0.156	1388
7	65.1	4	1	154.75	181	1524	1453	0.865	0.135	1338	0.009	0.991	0.134	1350
7	65.1	4	2	156.25	239	1524	1453	0.839	0.161	1490	0.012	0.988	0.159	1508
7	65.1	4	3	157.75	219	1524	1453	0.834	0.166	1318	0.008	0.992	0.165	1329
7	65.1	4	4	159.25	221	1524	1453	0.833	0.167	1321	0.007	0.993	0.166	1330
7	65.1	4	5	160.75	213	1524	1453	0.854	0.146	1461	0.008	0.992	0.145	1473

TABLE 1 – *Continued*

Leg	Hole	Core	Section	Depth Below Sea Floor (Meters)	γ^a Gamma Radiation	Mean Water Control	Mean Air Control	ϕ Porosity Fraction	1-ϕ Solid Fraction	$\gamma/(1-\phi)$	CO_3 Weight Fraction	1-CO_3 Weight Fraction	(1-ϕ)(1-CO_3) Weight Fraction	$\gamma/(1-\phi)(1-CO_3)$
Site 65 – *Continued*														
7	65.1	4	6	162.25	194	1524	1453	0.862	0.138	1409	0.010	0.990	0.136	1424
7	65.1	5	1	162.75	259	1518	1432	0.799	0.201	1290	0.019	0.981	0.197	1315
7	65.1	5	2	164.25	211	1518	1432	0.846	0.154	1370	0.009	0.991	0.152	1383
7	65.1	5	3	165.75	222	1518	1432	0.832	0.168	1323	0.010	0.990	0.166	1337
7	65.1	5	4	167.25	263	1518	1432	0.820	0.179	1472	0.007	0.993	0.178	1432
Site 66														
7	66	2	1	79.75	245	1489	1458	0.920	0.080	3076	0	1.000	0.080	3076
7	66	2	2	81.25	220	1489	1458	0.927	0.073	3014	0	1.000	0.073	3014
7	66	2	3	82.75	210	1489	1458	0.938	0.062	3378	0	1.000	0.062	3378
7	66	3	1	117.75	273	1512	1448	0.881	0.119	2296	0	1.000	0.119	2297
7	66	3	2	119.25	257	1512	1448	0.858	0.142	1814	0.012	0.988	0.140	1836
7	66	3	3	120.75	312	1512	1448	0.870	0.130	2402	0	1.000	0.130	2402
7	66	3	6	125.25	332	1512	1448	0.879	0.121	2733	0	1.000	0.121	2733
7	66	6	1	165.75	1669	1511	1453	0.625	0.375	4449	0.002	0.998	0.374	4458
7	66	6	2	167.25	1782	1511	1453	0.708	0.292	6111	0.001	0.999	0.291	6117
7	66	6	3	168.75	1917	1511	1453	0.700	0.300	6397	0.002	0.998	0.299	6410
7	66	6	4	170.25	2002	1511	1453	0.679	0.321	6235	0	1.000	0.321	6235
7	66	7	1	174.75	1867	1509	1421	0.691	0.309	6033	0.002	0.998	0.309	6045
7	66	7	2	176.25	2202	1509	1421	0.658	0.342	6441	0.001	0.999	0.341	6448
7	66	7	3	177.75	2360	1509	1421	0.659	0.341	6926	0	1.000	0.341	6926
7	66	7	4	179.25	2186	1509	1421	0.649	0.351	6230	0.001	0.999	0.350	6236
7	66	8	1	180.75	2052	1538	1474	0.709	0.291	7061	0	1.000	0.291	7061
7	66	8	2	182.25	1831	1538	1474	0.728	0.274	6679	0	1.000	0.274	6679
7	66	8	3	183.75	1767	1506	1428	0.774	0.226	7806	0	1.000	0.226	7806

TABLE 1 – *Continued*

Leg	Hole	Core	Section	Depth Below Sea Floor (Meters)	γ[a] Gamma Radiation	Mean Water Control	Mean Air Control	ϕ Porosity Fraction	1-ϕ Solid Fraction	$\gamma/(1-\phi)$	CO_3 Weight Fraction	1-CO_3 Weight Fraction	$(1-\phi)(1-CO_3)$ Weight Fraction	$\gamma/(1-\phi)(1-CO_3)$
Site 66 – *Continued*														
7	66	8	4	185.25	1597	1506	1428	0.799	0.201	7930	0	1.000	0.201	7903
7	66	8	5	186.75	1633	1506	1428	0.798	0.204	8016	0	1.000	0.204	8016
7	66	9	1	187.75	855	1496	1448	0.762	0.238	3592	0	1.000	0.238	3592
7	66	9	3	190.75	948	1496	1448	0.777	0.223	4250	0.002	0.998	0.223	4258
7	66.1	2	2	22.25	341	1483	1498	0.901	0.099	3463	0.006	0.994	0.098	3484
7	66.1	2	3	23.75	349	1483	1498	0.909	0.091	3837	0	1.000	0.091	3837
7	66.1	2	4	25.25	321	1483	1498	0.903	0.097	3318	0	1.000	0.097	3318
7	66.1	2	5	26.75	241	1483	1498	0.905	0.095	2539	0.005	0.995	0.095	2551
7	66.1	2	6	28.25	281	1483	1498	0.912	0.088	3192	0.009	0.991	0.087	3221
7	66.1	3	2	31.25	268	1521	1438	0.875	0.125	2143	0.002	0.998	0.125	2147
7	66.1	3	3	32.75	287	1521	1438	0.864	0.136	2109	0	1.000	0.136	2109
7	66.1	3	4	34.25	296	1521	1438	0.850	0.150	1978	0	1.000	0.150	1978
7	66.1	3	5	35.75	266	1521	1438	0.866	0.134	1985	0	1.000	0.134	1985
7	66.1	3	6	37.25	251	1521	1438	0.865	0.135	1851	0	1.000	0.135	1851
7	66.1	4	1	38.75	227	1512	1448	0.860	0.140	1620	0	1.000	0.140	1620
7	66.1	4	2	40.25	248	1512	1448	0.881	0.119	2084	0	1.000	0.119	2084
7	66.1	4	3	41.75	237	1512	1448	0.881	0.119	1989	0	1.000	0.119	1939
7	66.1	4	4	43.25	278	1512	1448	0.893	0.107	2601	0	1.000	0.107	2601
7	66.1	4	5	44.75	238	1512	1448	0.902	0.098	2424	0	1.000	0.098	2424
7	66.1	4	6	46.25	150	1512	1448	0.893	0.107	1398	0	1.000	0.107	1398
7	66.1	5	1	47.75	281	1526	1456	0.864	0.136	2068	0	1.000	0.136	2068
7	66.1	5	2	49.25	284	1526	1456	0.874	0.126	2256	0	1.000	0.126	2256
7	66.1	5	3	50.75	291	1526	1456	0.887	0.113	2568	0.012	0.988	0.112	2599
7	66.1	5	4	52.25	284	1526	1456	0.872	0.128	2220	0	1.000	0.128	2220
7	66.1	5	5	53.75	285	1526	1456	0.872	0.128	2228	0	1.000	0.128	2228
7	66.1	5	6	55.25	248	1526	1456	0.883	0.117	2126	0	1.000	0.117	2126

TABLE 1 – *Continued*

Leg	Hole	Core	Section	Depth Below Sea Floor (Meters)	γ[a] Gamma Radiation	Mean Water Control	Mean Air Control	ϕ Porosity Fraction	1-ϕ Solid Fraction	$\gamma/(1-\phi)$	CO_3 Weight Fraction	1-CO_3 Weight Fraction	$(1-\phi)(1-CO_3)$ Weight Fraction	$\gamma/(1-\phi)(1-CO_3)$
Site 66 – *Continued*														
7	66.1	6	2	58.25	258	1510	1434	0.889	0.111	2324	0	1.000	0.111	2324
7	66.1	6	3	59.75	293	1510	1434	0.878	0.122	2403	0	1.000	0.122	2403
7	66.1	6	4	61.25	313	1510	1434	0.867	0.133	2360	0	1.000	0.133	2360
7	66.1	6	5	62.75	294	1510	1434	0.873	0.127	2309	0	1.000	0.127	2309
7	66.1	6	6	64.25	253	1510	1434	0.869	0.131	1934	0	1.000	0.131	1934
7	66.1	7	1	67.75	312	1527	1424	0.903	0.107	3226	0	1.000	0.097	3226
7	66.1	7	2	69.25	302	1527	1424	0.886	0.114	2646	0	1.000	0.114	2646
7	66.1	7	3	70.75	279	1527	1424	0.859	0.141	1970	0.011	0.989	0.141	1992
7	66.1	7	4	72.25	299	1527	1424	0.869	0.131	2290	0	1.000	0.131	2290
7	66.1	7	5	73.75	276	1527	1424	0.850	0.150	1842	0	1.000	0.150	1842
7	66.1	7	6	75.25	288	1527	1424	0.887	0.113	2545	0	1.000	0.113	2545
7	66.1	8	1	75.75	286	1522	1476	0.868	0.132	2169	0	1.000	0.132	2169
7	66.1	8	2	78.25	308	1522	1476	0.859	0.141	2195	0.001	0.999	0.140	2197
7	66.1	8	3	79.75	309	1522	1476	0.874	0.126	2461	0	1.000	0.126	2461
7	66.1	8	6	84.25	298	1522	1476	0.865	0.135	2211	0	1.000	0.135	2211

[a]Arithmetic mean of counts of middle 16 of 20 three-inch intervals per section in [counts/3"/1.25 minutes] - 1350 background.

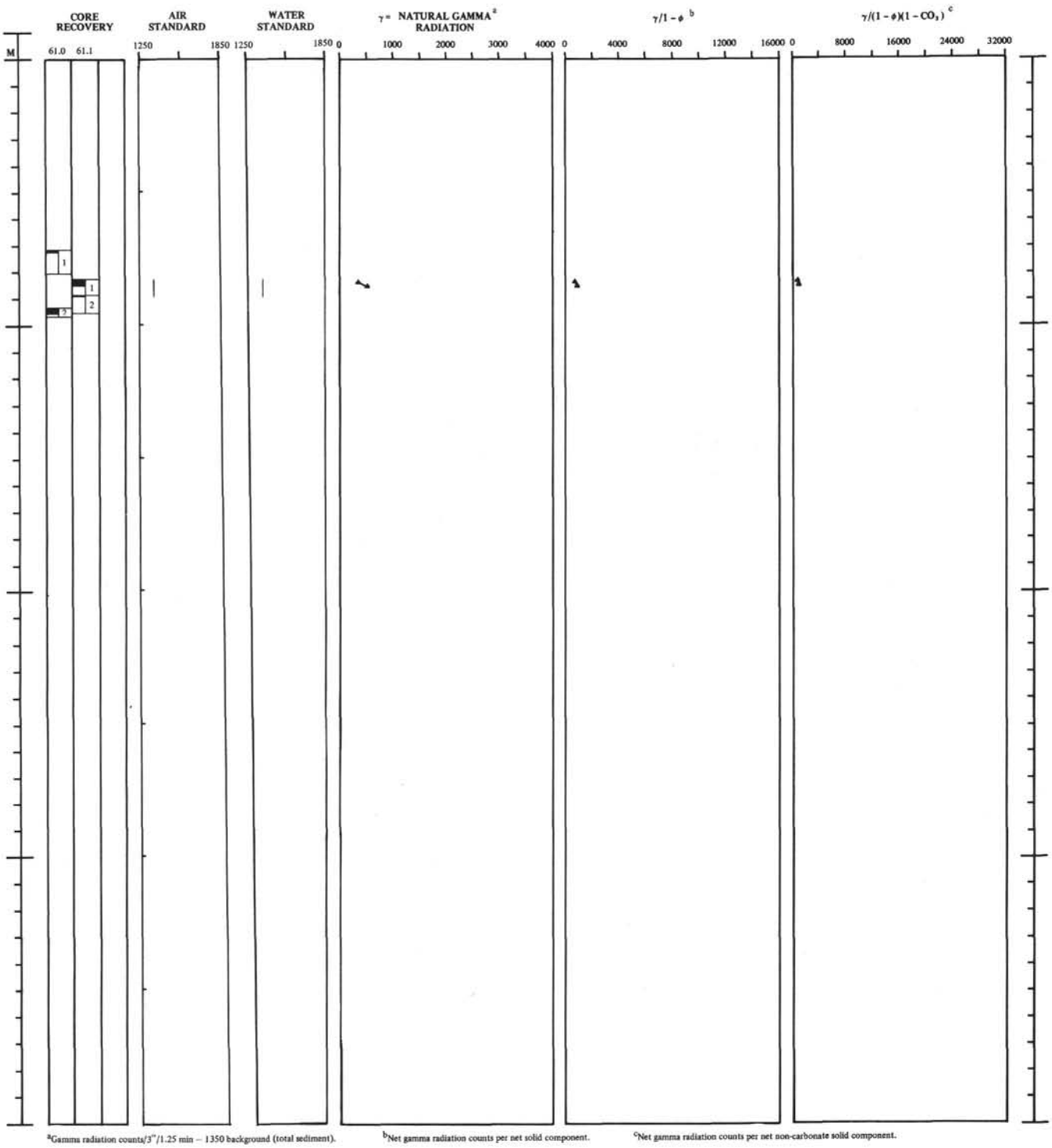

gure 1. *Natural gamma radiation, Site 61.*

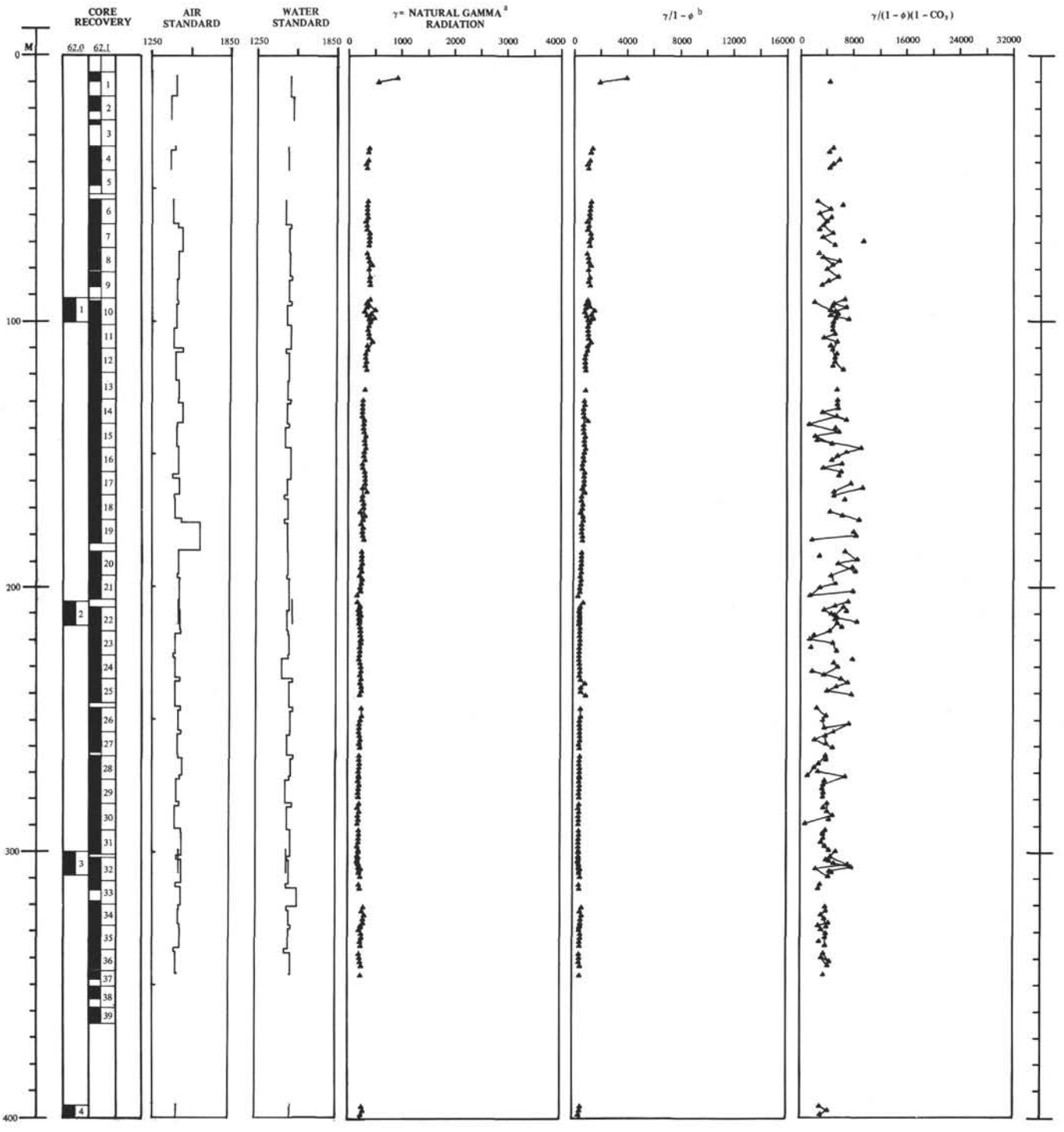

Figure 2. *Natural gamma radiation, Site 62.*

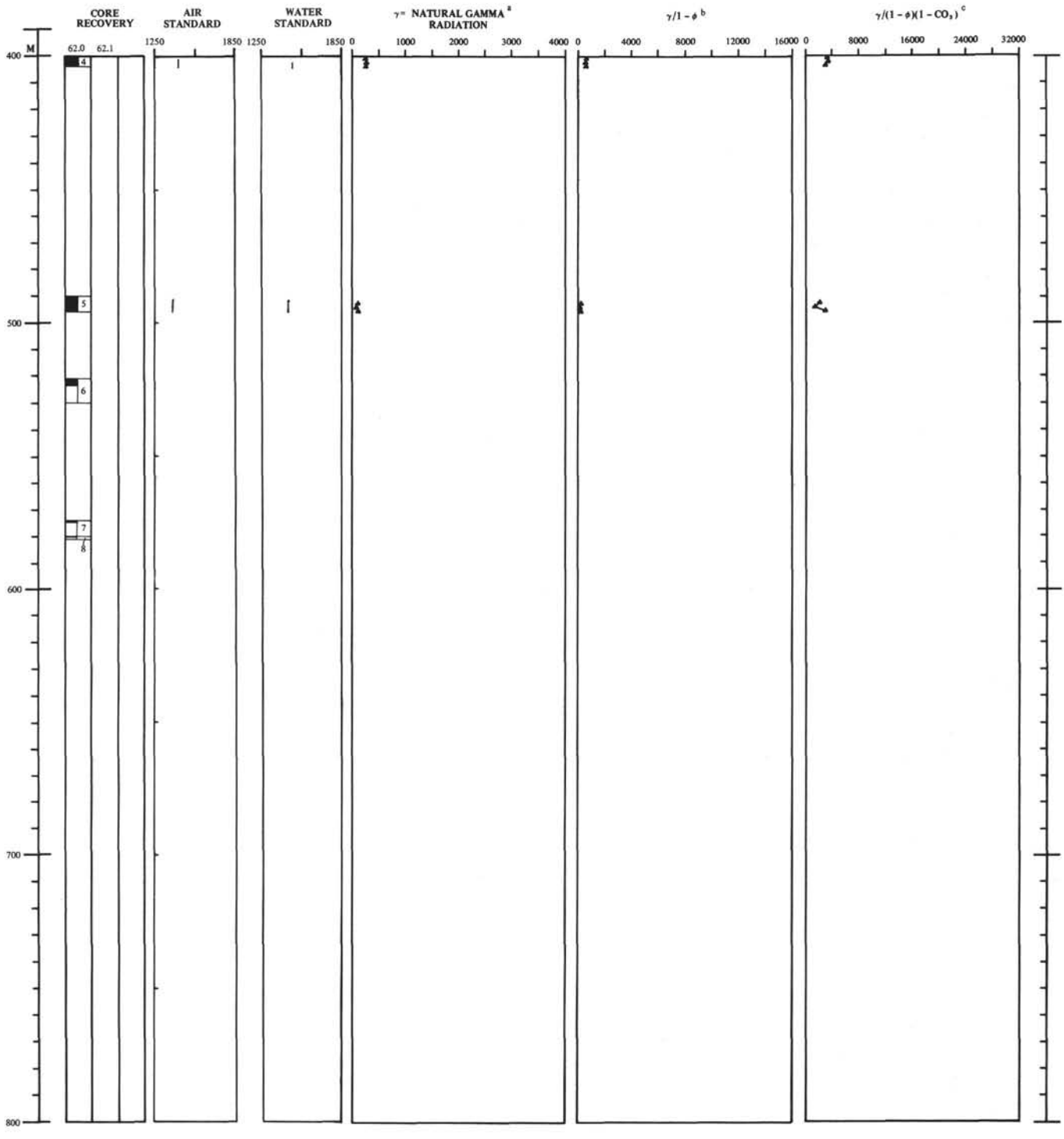

Figure 2. *Continued.*

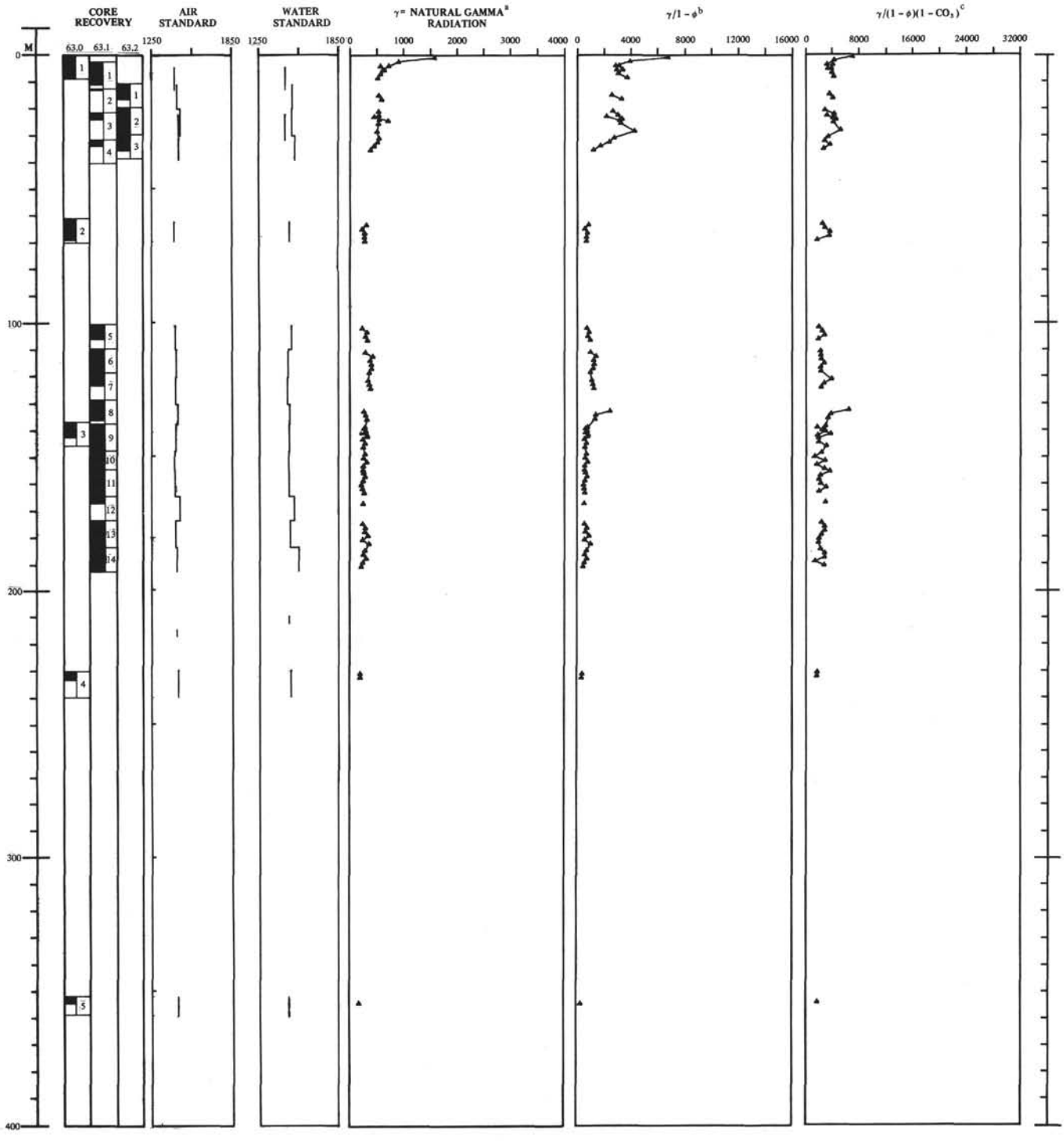

Figure 3. *Natural gamma radiation, Site 63.*

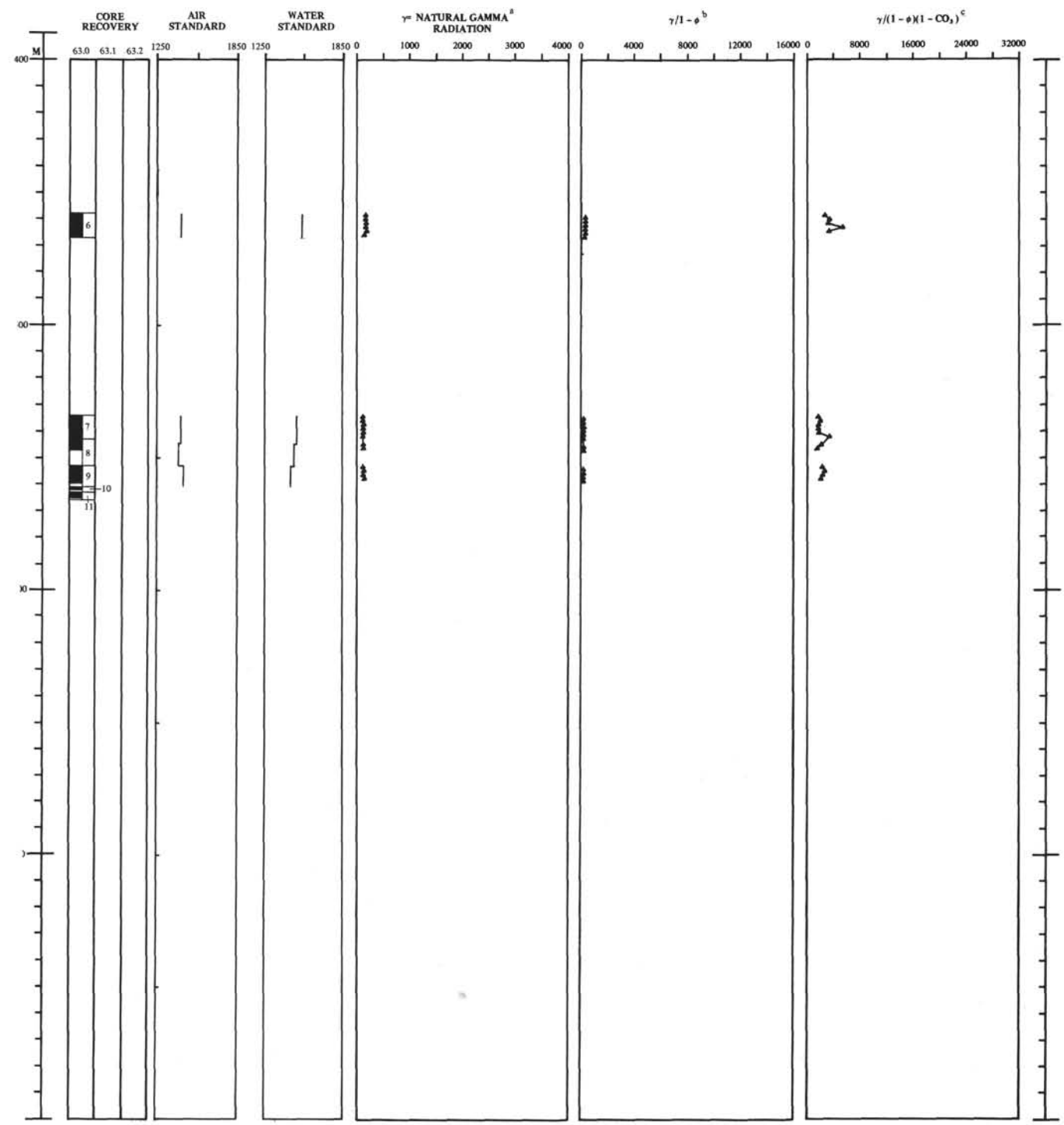

gure 3. *Continued.*

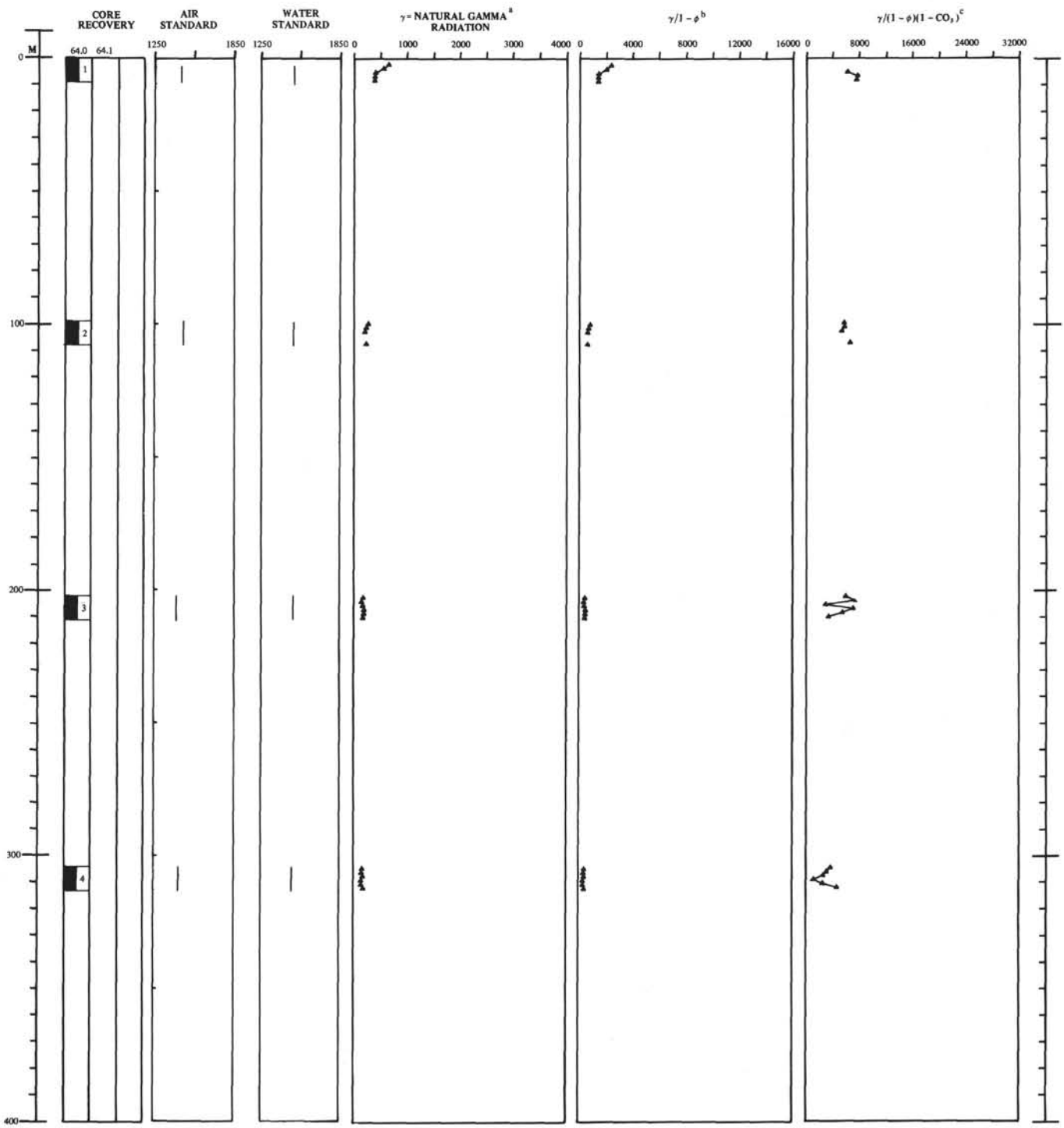

Figure 4. *Natural gamma radiation, Site 64.*

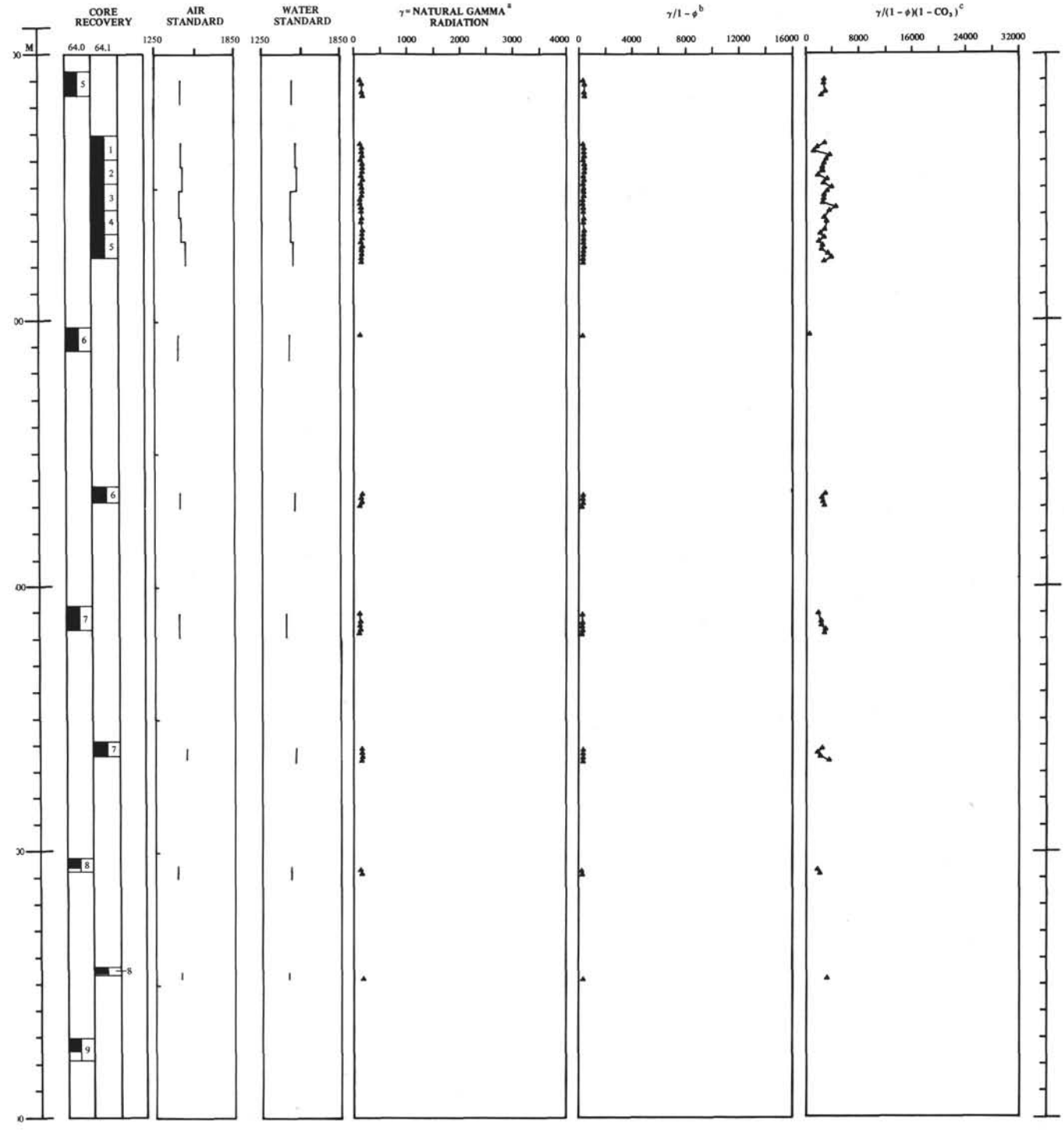

Figure 4. *Continued.*

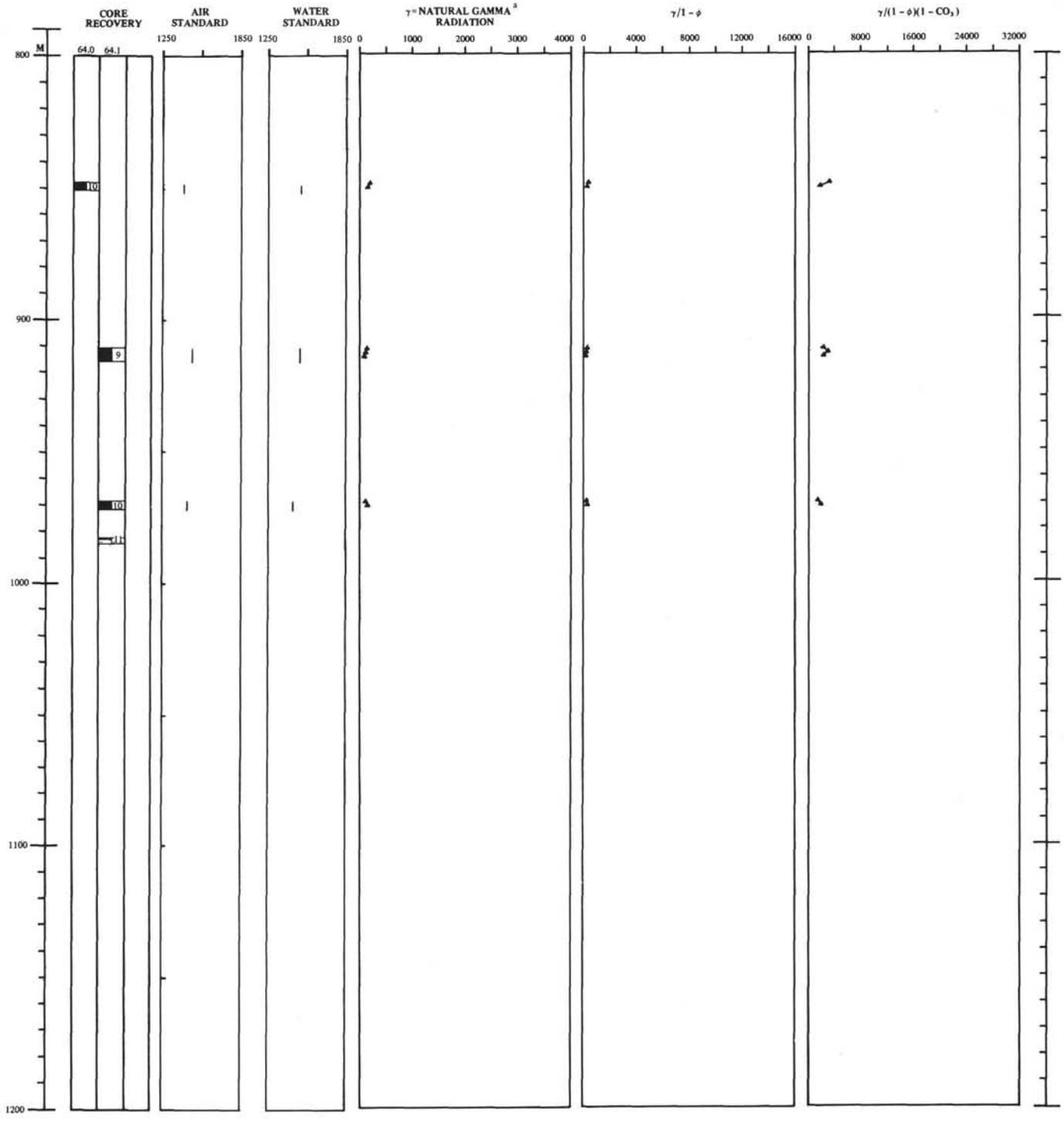

Figure 4. *Continued.*

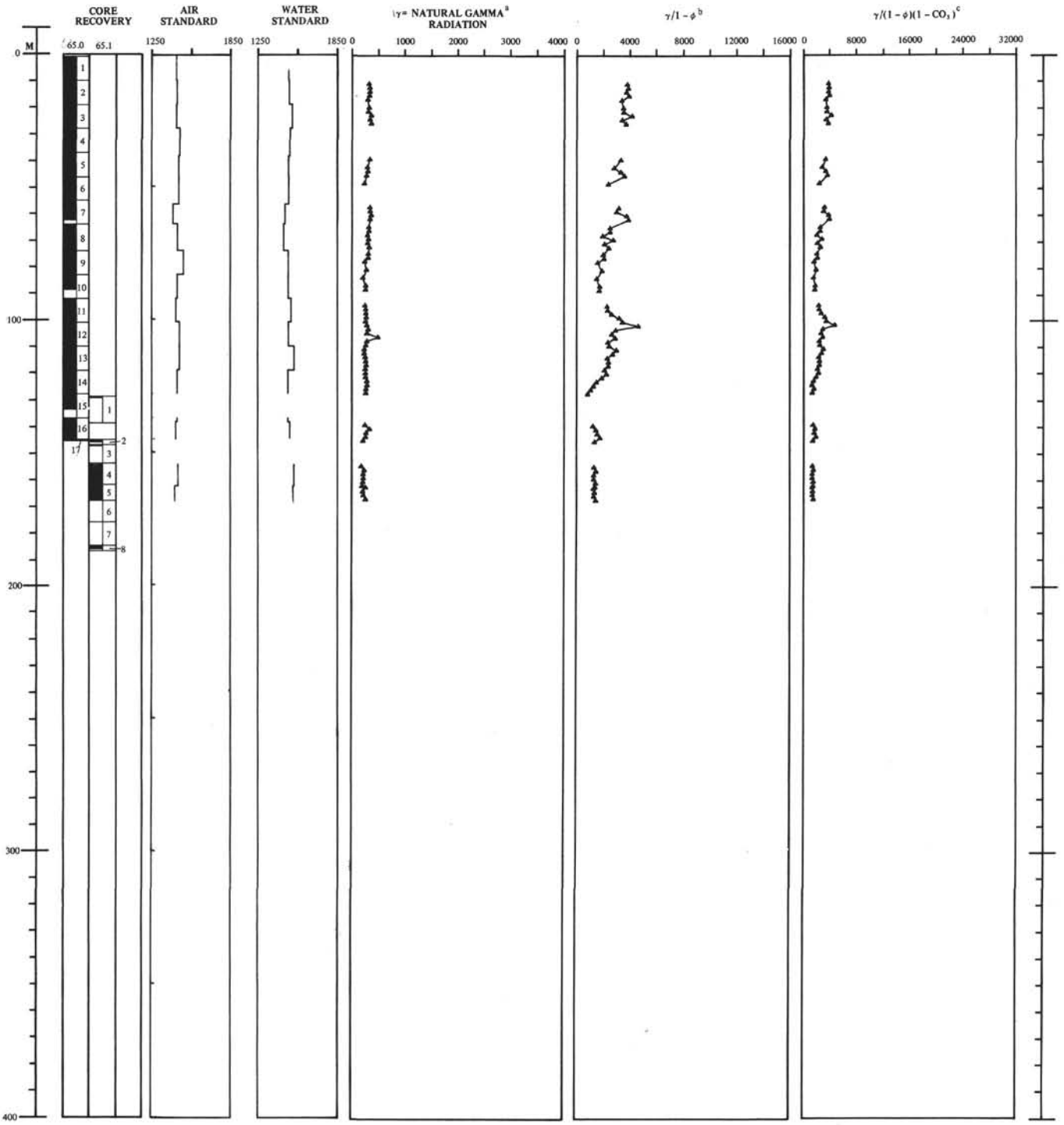

Figure 5. *Natural gamma radiation, Site 65.*

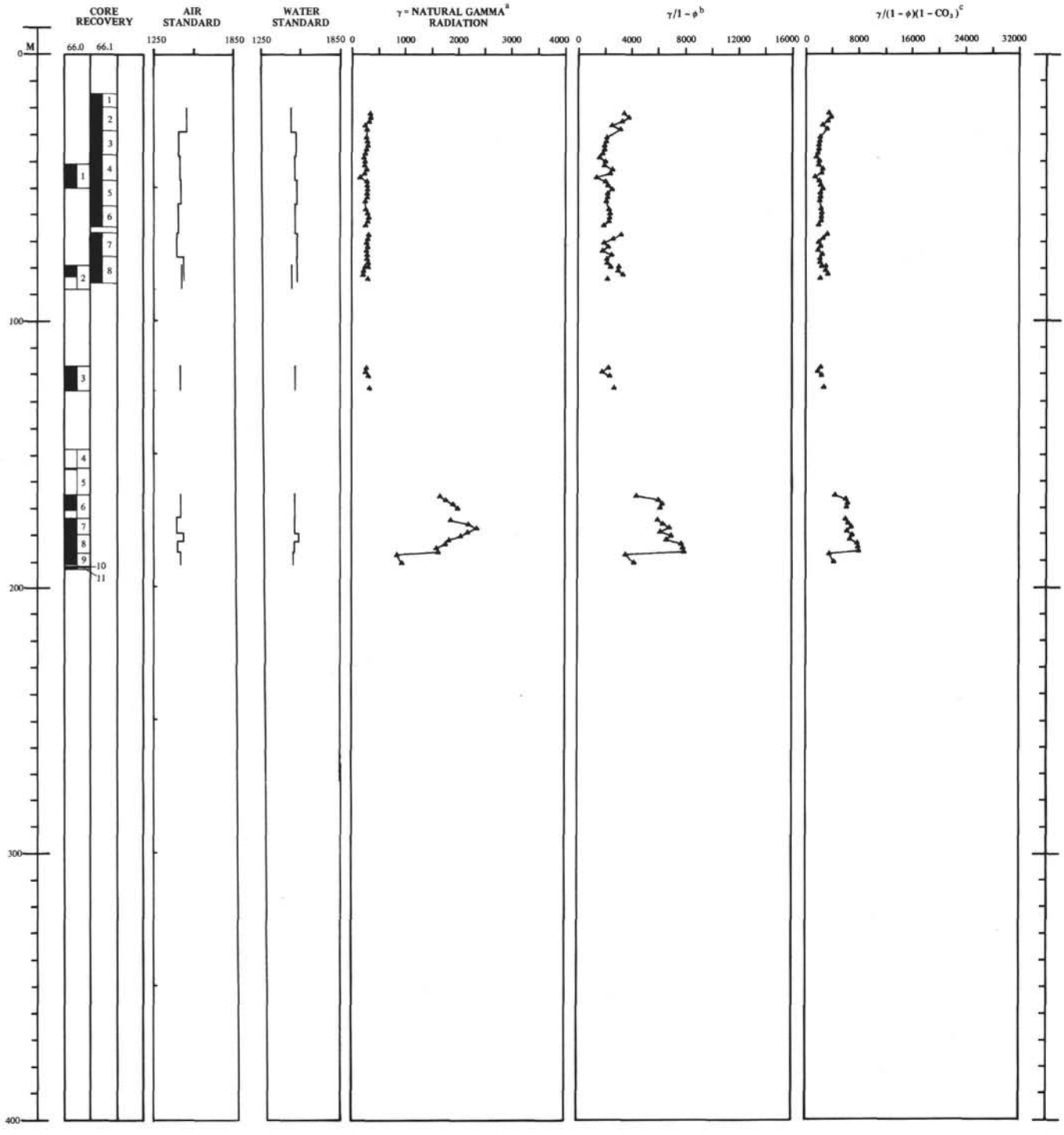

Figure 6. *Natural gamma radiation, Site 66.*

correlated with natural gamma radiation measurement on cores, it was found that:

$$\gamma_C = 1350 + 40.80\gamma_L$$

where γ_C is in counts /3 X 0.4-inch core/1.25 minutes, and γ_L is in API units, At Site 29, the mean air control values ranged from 1365 to 1582 counts, a range similar to that obtained on Leg 7. The difference between the derived background value of 1350 from Site 29 data and the air control values may represent the shielding effect of the core material itself.

The uncertain reliability of the controls run in connection with gamma radiation measurements made aboard the D /V *Glomar Challenger* poses a problem in the selection of a background count by which raw measurements should be reduced. That the system is counting energy from sources other than from the sediment cores is clear. That the cores themselves provide some shielding against extraneous radiation in the laboratory seems likely. Attenuation of only seven per cent of the gamma rays providing the air background count of 1450 would result in the background count of 1350 derived from Leg 4 data. Because variations in the controls appear not to be reflected in the measurements on the cores themselves, we have elected to subtract a constant from the raw data, rather than either of the controls measured between cores. Further, because of the possible shielding effect of the cored materials, we have elected to subtract the minimum value of 1350 counts/1.25 minutes rather than the median values of either the water or air controls.

Thus, all raw gamma-ray data collected on Leg 7 in total counts have been corrected by subtracting a value of 1350 counts, and these corrected values are designated net counts. Net gamma ray counts are shown as a function of depth on the Core description Charts and the Site Summaries in Chapters 3 through 9. Values of net gamma counts as a function of depth are also shown on Figures 1 through 6 of this chapter.

The average of the net gamma-ray counts of the middle 16 to 20 increments in each section scanned were averaged. These averages are plotted on Figures 1 through 6 and are listed in Table 1. Values of average net gamma radiation are repeated in the tables of physical and chemical properties at the end of Chapters 3 through 9.

Like other down-hole gamma ray tools in current use, the gamma ray tool used on Leg 4 was calibrated in test pits maintained by the American Petroleum Institute (A.P.I., 1959; W. B. Belknap *et al.*, 1966). The tools are calibrated in API units wherein the tool response is set to zero in a nonradioactive pit, and set to respond about 11.7 API units for each microgram of radium equivalent per metric ton.

If γ_R = natural gamma ray radiation of 1 microgram radium equivalent per ton,

and $\gamma_R = 11.7\,\gamma_L$

and $\gamma_C = 1350 + 40.8\,\gamma_L$,

then $\gamma_R = .2878\,\gamma_C - 387.$

The following concentrations of radioactive materials give about the same response as one microgram of radium per ton: 2.8 ppm uranium, 3.5 ppm thorium, and 2000 ppm potassium.

The volume of the sediment mass to which the natural gamma scanner is responding is uncertain. If it responds to the entire volume and only to the volume represented ny the 2.5-inch diameter core, 3 inches in length, 322 cubic centimeters are involved. Not considering attenuation by core materials, a net count of 650 would require a concentration of 2.65 per cent potassium, which is not unreasonable for some marine clays.

The amount of attenuation of the natural gamma radiation provided by the core material itself cannot be known in the absence of information about the energy spectra. However, if the gamma radiation is from the decay of K^{40}, at least 70 to 80 per cent of quanta with the original energy should be recorded by the crystals (Figures 11 and 12). This estimate is based on the following assumptions:

1) the photon energy of the radiation is 1.4 Mev;

2) the source of the radiation is a line at the axis of the cylindrical core;

3) the radius of the core is 3.125 centimeters;

4) the centimeters of material necessary to reduce the gamma rays by a factor of two is (after L. Slack, and K. Way, 1959):

water (ρ = 1.00 gm/cm^3) : $T_{1/2}$ = 11.7 centimeters;

concrete (ρ = 2.35 gm/cm^3) : $T_{1/2}$ = 5.5 centimeters;

lead (ρ = 11.29 gm/cm^3) : $T_{1/2}$ = 1.15 centimeters.

In actual fact, many of the attenuated gamma rays will reach the crystals and be counted, and the fractions shown on Figures 11 and 12 should be considered

minimum values only. Half thicknesses in grams per square centimeters can be derived from the relationship:

$$T_{1/2}\ (gm/cm^2) = T_{1/2}\ (cm)\ \rho\ (gm/cm^3).$$

RESULTS

Relationship between Natural Gamma Radiation and Solid Fraction

It can be observed (Site Summaries, Chapters 3 through 9) that over short stratigraphic intervals the natural gamma radiation tends to decrease with an increase in porosity. In order to test the hypothesis that gamma ray producing elements may be confined largely to the solid phase of these marine sediments, the average net gamma count per section was plotted against the proportion of the total sediment occupied by solid constituents (1-0). The relationships for all sections at each site are shown on Figure 7; the relationships for all sections at all sites is shown on Figure 8.

A least squares regression of the data yields an equation of the form:

$$Y = A X + B$$

where $X = (1-\phi)$, or the net solid component

and $Y \times 10^3$ = net gamma counts/1.25 minutes

which was calculated for all pairs of samples at Sites 62, 63, 64, 65 and 66 and for pairs at all of these sites. The standard deviation of A and B and the standard error of estimate for X and Y were determined, (Table 2). Lines determined by least squares regression are shown on Figures 7 and 8. Statistical techniques are after Dixon and Massey (1957).

Of the comparisons of arrays, those from Sites 62, 63 and 64—where lithologies are similar and the range of net solid components relatively wide—are most credible. The least squares regressions of the other arrays are of questionable value: Data from Site 66 are from both the radiolarian ooze and the pelagic clay; similarly, the composite least squares regression includes data from several different lithologies. Because of the very narrow range of net solid fraction of the radiolarian ooze from Sites 65 and 66, the least squares regression of these data is questionable. Values of net solid fraction are from about 0.10 to 0.20 and the standard error of estimate for (1-0) in the radiolarian ooze at Site 65 is 0.05.

Data from Sites 62, 63 and 64 show a decrease in gamma radiation with increase in fraction of solid components, which is in conflict with the observation over short intervals mentioned above. This decrease probably does not indicate a direct relationship, but may result from the fact that an overall decrease in natural gamma radiation with age is noted in rocks of similar type cored on this leg, and the fact that there is a general decrease in porosity with depth.

The net gamma count of the solid fraction of the sediments is listed for each section in Table 1, and is shown plotted as a function of depth in Figures 1 through 6.

Gamma radiation of the net solid component displayed as a function of depth (Figures 1 through 6) shows a similar pattern at Sites 62, 63 and 64. The radiolarian ooze penetrated at Site 65 and Site 66 shows a much lower gamma radiation to solid fraction ratio than calcareous oozes of similar porosity. However, the gamma radiation of the pelagic clay penetrated at Site 66 is markedly higher (X 7) than that of either the radiolarian oozes or the calcareous oozes of similar porosity. According to Dreever (Chapter 17, this volume) the clay consists of about 40 per cent palygorskite, 30 per cent mica, 20 per cent montimorillonite, 5 per cent kaolinite and chlorite, and 3 per cent quartz.

Relationship between Natural Gamma Radiation and Noncarbonate Solid Component

Arrhenius and Goldberg (1955) note that the beta activity of a pelagic carbonate sediment based on its calcium-carbonate free weight is similar to that of nearby carbonate free pelagic clays. To test whether the radionuclides in these marine sediments might be confined largely to the noncarbonate solid component, the average net gamma count per section was plotted against the total net noncarbonate solid fraction of the section $[\gamma net/(1 - 0)\ (1 - CaCO_3)]$, and the results for sediments at Sites 62, 63 and 64 are shown on Figure 8.

Sites 62, 63 and 64 were selected because most of the biogenous component in the cores consists of calcium carbonate.

A least squares regression of the data yields an equation of the form:

$$Y = A X + B$$

where $X = (1-\phi)\ (1-CO_3)$ or, net noncarbonate solid component

and $Y \times 10^3$ = net gamma ray counts/1.25 minutes

which was calculated for all pairs of samples at Sites 62, 63 and 64 and for all pairs at all of these sites. The standard deviation of A and B and the standard error of estimate for X and Y were determined, (Table 3). Lines determined by least squares regression are shown on Figure 9.

TABLE 2
Comparison of Arrays of Values of Net Solid Component and Net Gamma Count

Site	Dominant Lithology	No. Pts.	Values of A and B Calculated by Least Squares Regression for $Y = A X + B$				Standard Error of Estimate	
			A		B		X	Y
			Value	Standard Deviation	Value	Standard Deviation		
62	Chalk ooze	194	-0.8586	0.0146	+0.6181	0.0363	0.0584	0.0681
63	Chalk ooze	94	-1.0455	0.0201	+0.7248	0.0503	0.0755	0.0722
64	Chalk ooze	76	-0.7331	0.0170	+0.4814	0.0384	0.0326	0.0445
65	Radiolarian ooze	70	-0.2245	0.0085	+0.3176	0.0605	0.0499	0.2220
66	Radiolarian ooze and pelagic clay	59	+8.0682	0.0322	-0.6419	0.1789	0.2319	0.0287
Composite, Sites 62, 63, 64, 65 and 66		493	-0.4365	0.0153	+0.4624	0.0422	0.2853	0.6536

TABLE 3
Comparison of Arrays of Values of Net Noncarbonate Solid Component and Average Net Gamma Count

Site	Dominant Lithology	No. Pts.	Values of A and B Calculated by Least Squares Regression for $Y = A X + B$				Standard Error of Estimate	
			A		B		X	Y
			Value	Standard Deviation	Value	Standard Deviation		
62	Chalk-ooze	194	+0.6760	0.0052	+0.2289	0.0675	0.0704	0.1042
63	Chalk-ooze	94	+3.0712	0.0193	-0.0269	0.1545	0.1075	0.0350
64	Chalk-ooze	76	-0.1876	0.0063	+0.1707	0.0972	0.0383	0.2042
62, 63, 64 (Composite)		384	+1.6453	0.0056	+0.1358	0.0622	0.1115	0.0678

Scatter in these data are high, which is not surprising considering the laboratory difficulties in measuring carbonate (see chapter on carbonate content, this volume) and the generally low level of gamma radiation of these cores. Furthermore, the overall decrease in net gamma radiation with depth undoubtedly obscures any relationship between net gamma count and net noncarbonate solid fraction. Nevertheless, it does appear that there is a correlation: the net gamma radiation increases in general with increased net noncarbonate solid fraction of the sediments.

The net gamma count of the noncarbonate solid fraction of the sediments [γnet/ (1 - 0) (1 CO_3)] is listed for each section from Sites 62, 63 and 64 in Table 1, and is shown plotted as function of depth for these sites in Figures 1 through 6. The net gamma count of the noncarbonate solid fraction for Sites 62, 63 and 64 is somewhat lower but of the same order of magnitude as that of the net solid fraction of the pelagic clay penetrated at Site 66. Values from Site 62 range from 1370 counts near the surface to 2000 counts at about 500 meters; values from Site 63 range from 4190 counts near the surface of 2400 counts at 560 meters; and values from Site 64 range from 12,500 counts near the surface to 1790 counts at 970 meters. Values of net gamma radiation of the net solid fraction of the pelagic clay at Site 66 range from 6000 to 8000 counts.

RESULTS

Natural Gamma Radiation of Cores from Site 61

At Site 61 only 7 meters of core were recovered, and only Sections 1 and 2 of Core 61.1-1 were undisturbed enough to justify measuring natural gamma radiation. The cores were of an Upper Cretaceous stiff clay containing fragments of consolidated porcelanite. The mean net gamma count of Section 61.1-1-1 was 344, and that of Section 61.1-1-2 was 519 (Figure 1).

Natural Gamma Radiation from Site 62

Holes at Site 62 penetrated 581 meters of very pure nannofossil ooze-chalk with a sugary dolomite at the base. Sediments ranged in age from Quaternary to Late Oligocene. Almost all sections retrieved from both Holes 62.0 and 62.1 were scanned and a composite from the two sites yields a good profile (Figure 2) from a depth of 5 meters to the total depth of 581 meters.

Three zones are detectable on the profile of total net gamma radiation: The first is a Late Quaternary zone of higher radioactivity (as high as an average of 918 counts in Section 62.1-1-2). The top of the second zone is between 10 and 35 meters below the sea floor (early Quaternary) and extends to 110 meters (Early Pliocene), where radioactivity is moderate (about 375 counts). In the third zone the radioactivity decreases steadily from about 330 at a depth of 120 meters (Early Pliocene) to about 105 counts at 490 meters (Early Miocene). The higher counts in the two upper zones may be related in part to lower carbonate content: The carbonate content averages about 60 per cent in the upper zone, about 75 per cent in the middle zone, and about 85 per cent in the lower zone.

Net gamma radiation exceeds 650 net counts at the following horizons: 62.1-1-2, entire section >650 net counts; 62.1-1-3, 23-30 centimeters; 62.1-1-3, 84-91 centimeters; 62.1-1-3, 99-106 centimeters; 62.1-10-3, 38-61 centimeters; and, 62.1-10-5, 137-150 centimeters.

These layers are probably more radioactive because they contain more volcanogenic material. Volcanic glass was noted (rare or common) in smear slides from Hole 62.0 (Cores 1, 2, 3, 4, 7, 8, 9, 10, 11 and 15) and from Hole 62.1 (Cores 2, 3 and 5) but no systematic investigation was made to determine the correlation between natural gamma radiation and volcanogenic content.

The net gamma radiation to net solid fraction also shows high radioactivity in the near surface Quaternary. It decreases steadily from 1370 counts at 35 meters beneath the sea floor to 200 counts at 500 meters, a decrease of 60 counts/M.Y. Fifty per cent of the net gamma radiation (on a net solid basis) is lost after about 11 million years.

The net gamma radiation to net noncarbonate solid fraction increases slightly from about 5000 counts at 35 meters beneath the seafloor to 5600 counts at 130 meters. Late Miocene sediments show both a generally higher gamma count (the average net counts of several sections exceeds 8000 counts) and there is more scatter in these data than in older and younger sediments. Below this interval, the net noncarbonate solid component shows a more or less steady decrease in gamma radiation from 3500 counts at 250 meters to 2000 counts at 500 meters.

Natural Gamma Radiation of Cores from Site 63

Three holes at Site 63 penetrated 566 meters of sediment consisting of about 30 meters of Quaternary Pliocene pelagic clay and marl overlying a very pure nannofossil ooze chalk ranging in age from Late Miocene to Early Oligocene. The upper thirty meters and the interval between 100 and 190 meters were cored continuously, but the rest of the section was cored only about once each 100 meters.

Despite the incomplete coverage, several zones of radioactivity can be noted. Cores from the Pliocene-Quaternary marl-clay sequence are highly radioactive. The uppermost section just below the sea floor shows an average of 1580 net counts; the remainder of the section shows about 500 net counts. Cores from the underlying Miocene nannofossil chalk ooze show a relatively constant gamma radiation of about 250 net counts throughout most of the section. The interval between 100 and 125 meters is slightly more radioactive (as high as 428) and the cores at 230 meters show a net gamma radiation of only 193 counts. Below this the net gamma radiation decreases steadily from 193 counts at 230 meters to about 130 counts at 555 meters.

The net gamma radiation to net solid fraction is also high in cores from the Pliocene-Quaternary marl-clay sequence. The uppermost section shows an average of 6775 net counts, and cores from the remainder of the sequence about 3000 counts. Below this interval, the net solid fraction shows a steady decrease from about 670 counts at 65 meters to 215 counts at 555 meters, except for one Middle Miocene interval between 110 and 135 meters which shows a net count of about 1280.

Except for a layer at the surface and at 135 meters—which show higher values, the net gamma radiation to net noncarbonate solid fraction shows a steady decrease in net gamma count from 4190 counts at about 10 meters to 1770 counts at 355 meters, in the Upper

Oligocene. Average net gamma counts of the net noncarbonate solid fraction of cores from the interval below 355 meters are generally higher: about 3450 counts at 460 meters, and about 2400 counts in the interval between 535 to 560 meters.

Natural Gamma Radiation of Cores from Site 64

Holes drilled at Site 64 penetrated 985 meters of very pure nannofossil chalk ooze ranging in age from Quaternary to Middle Eocene.

As at Sites 62 and 63, the near surface sediments are more radioactive. Measurements on cores indicate that radioactivity of the ooze decreases steadily from an average of 230 net counts at 100 meters beneath the sea floor (Lower Pliocene) to 122 net counts at 500 meters (Lower Miocene). Below this the net gamma count is nearly constant to the total depth.

The net gamma radiation to solid fraction is also high for cores taken in the first 7 meters. Below this interval, the net gamma counts to solid fraction decrease steadily from 660 net counts at 100 meters to 270 counts at 500 meters. Below this, the net gamma counts to solid fraction remains relatively constant to the total depth.

The net gamma radiation to net noncarbonate solid fraction is also high above 7 meters (12,500 counts). Below this it decreases irregularly with depth from 7500 at 10 meters, to 5500 at 100 meters, to 5400 at at 200 meters, to 3000 at 300 meters. Below 300 meters the ratio remains about the same to a depth of 750 meters. Below this it decreases steadily to 1790 counts at a depth of 970 meters.

Natural Gamma Radiation of Cores from Site 65

Holes at Site 65 penetrated 187 meters of radiolarian ooze ranging in age from Quaternary to Middle Eocene.

The average net gamma radiation of cores from the radiolarian ooze decreases steadily from 340 counts at 10 meters to 225 counts at 160 meters. One unusually radioactive section (65.0-12-4) had an average net count of 503. The surface sediments were not cored.

The average net gamma radiation to solid fraction decreases in a more erratic manner. At 10 meters the count is 3800 and it decreases more or less regularly through Pliocene and Upper Miocene sediments to about 3100 in a Middle Miocene ooze at 57 meters. Below this, the count decreases abruptly to 1600 at 85 meters. Near the Lower Miocene-Upper Oligocene boundary, the counts increase to an average of about 3000 counts, and it is this interval that contains the radioactive layer mentioned above. Below this boundary, the average net gamma counts decrease to about 1400 and are near this value in the underlying Eocene sediments.

Except for a few layers of nannofossil-radiolarian ooze and impure silicified limestone between 125 to 140 meters, sediments penetrated at Site 65 are almost devoid to carbonate. Thus, the values of average net gamma radiation to net noncarbonate solid fraction are similar to the values of net radiation to solid fraction.

Natural Gamma Radiation of Cores from Site 66

Holes drilled at Site 66 penetrated 165 meters of radiolarian ooze ranging in age from Quaternary to Early Miocene, overlying about 25 meters of stiff fine-grained pelagic clay, Cretaceous in age. The natural gamma radiation of the radiolarian ooze is uniformly low, about 300 average net counts throughout. The pelagic clay is highly radioactive, average net counts range from 1630 to 2350, except in the lowest part. The base of the clay is rich in ferromanganese oxides and volcanoclastic sands, and is less radioactive than the overlying clay, averaging 900 counts.

In the radiolarian ooze, the natural gamma radiation to net solid fraction decreases from about 3500 average net counts at 25 meters to 2000 average net counts at 35 meters, and then increases slightly to 2000 counts at 120 meters. Except for the uppermost section, and intervals rich in ferromanganese oxides at the base, the Cretaceous pelagic clay has a high net gamma count to net solid fraction and it increases from about 4500 counts at 16.5 meters. Several sections in the interval from 70 to 85 meters show over 3000 net counts/net solid fraction.

The sediments penetrated at Site 66 are almost devoid of carbonate, and therefore the values of average net gamma radiation to net noncarbonate solid fraction are almost identical to the values of net gamma radiation to net solid fraction.

DISCUSSION

One of the several dozen radioactive isotopes occurring in nature, those of the uranium, thorium and protactinium series and potassium-40 produce almost all of the natural gamma radiation of marine sediments (Frielander, *et al.*). All of the daughter isotopes of these decay series have half lives less than one million years except those of:

U^{238}: half life = 4.51×10^9 years;
U^{235}: half life = 7.13×10^8 years;
Th^{232}: half life = 1.41×10^{10} years;
K^{40}: half life = 1.25×10^9 years.

Studies of cores collected on Leg 7 show that where data exist, near surface sediments all have high natural gamma radiation. Values decrease rapidly to a depth equivalent to about 1 million year, where there is a break in the gradient of net gamma count displayed as a function of depth.

Cores of sediments recovered below this surface layer show a consistent and substantial reduction in natural gamma radiation with depth. For example, at Site 62 (Table 4) there is a loss of 69 per cent of the natural gamma radiation between 115 meters and 490 meters. On a total saturated sediment basis, 69 per cent of the natural gamma radiation is lost in 15 million years; on a dry basis, 77.5 per cent is lost.

Until the specific radioactive isotopes producing the gamma radiation and their ratios are determined, speculations concerning the observed decrease in gamma radiation are tenuous.

Some, but not all, of the reduction with depth in gamma radiation counted can be attributed to the increased attenuation of the gamma rays by the increase in density with depth (Figure 12). If the dominant radionuclide is K^{40}, an increase in density from 1.6 to 2.2 would result in a reduction in gamma rays counted of less than 10 per cent.

If the radioactive nuclides were confined to the interstitial water, the reduction in interstitial water content with depth would account for the decrease in natural gamma radiation with depth. However, at Site 62 a reduction in natural gamma radiation of 69 per cent from 115 meters to 490 meters parallels a reduction in porosity of only 22.6 per cent, which is insufficient to explain all of the reduction in radioactivity. Further, over short intervals, the natural gamma radiation appears to increase with a decrease in porosity.

The reduction in natural gamma radiation with depth cannot be due to the decay of radionuclides in the sediments. At Site 62, on a total saturated sediment basis, 50 per cent of the gamma radiation is lost after 10.8 million years; on a dry basis, 50 per cent is lost after 9.7 million years. The loss in radiation at Sites 63 and 64 also indicate a rate of loss of about 50 per cent per 10 million years. No radioactive nuclides known have a half life which approximates 10 million years.

Changes in Initial Radionuclide Content

The decrease in gamma radiation with age may be due, at least in part, to a gradual increase with time in the initial radioactivity of the sediments at accumulation. Both the amount of radionuclides delivered to the ocean water mass by subaerial erosion, and the conditions favorable to their incorporation into sediments could vary with time.

The first possibility is supported by a study of sediments at the Guadalupe Site. Chow, Tatsumoto and Patterson (1962) show that the composition of authigenic lead and biogenic lead in sediments from this site changes with time. They state that the older lead, which may have been derived primarily from predominantly basalt-surface drainage during the Middle Miocene, is less radioactive than the average lead in the oceans and that post Miocene lead (derived primarily from drainage from crystalline plutons or their sedimentary equivalents) is more radioactive.

With regard to the second possiblity, there is evidence that changes in bottom circulation may result in changes in radionuclide content of the bottom sediments. Arrhenius (1963) notes that phosphates accumulating under reducing conditions are high in uranium, whereas those accumulating under oxidizing conditions have a low uranium content.

Loss of Radionuclides by Leaching and Advection

The decrease in radioactivity with depth may reflect gradual leaching and removal of radionuclides by advection of interstitial fluids as the sediments compact. Some earlier studies tend to support this hypothesis.

Arrhenius and Goldberg (1955) analyzed a highly radioactive pelagic clay near the sediment surface, and found that the fine fraction, consisting largely of clay and hydroxide minerals, was as radioactive as a pure phillipsite fraction, in contrast to deeper pelagic clay samples, where the radioactivity was produced mostly by the coarser phillipsite-rich fractions. They conclude that a reduction in beta activity in the fine fraction with age resulted from leaching of unsupported ionium with time.

A study of recent and ancient carbonate sands by Haglund, Freedman and Miller (1969) shows that a consistent decrease in uranium content with consolidation occurs as aragonite and magnesium-rich calcite are removed.

Koczy (1954) found an excess of radium over ionium in seawater and attributed this excess to the addition of uranium to the ocean water mass by diffusion from near surface sediments. Work by Bernat and Goldberg (1969) shows that there are movements of Ra^{228} within the sedimentary column.

TABLE 4
Reduction of Natural Gamma Radiation with Depth at Site 62

Core	Depth (meters)	Age	γ_C	ρ_B	ϕ	$1-\phi$	$\frac{\gamma}{(1-\phi)}$
62.1-12	115	4.8 m.y.	335	1.67	0.62	0.38	880
62.0-5	490	19.5 m.y.	104	1.90	0.48	0.52	200
	375	15 m.y. ±	231 = 69%	14% or 22.6%			680 or 77.5%

FUTURE WORK

Two modifications in the natural gamma radiation program of the Deep Sea Drilling Project in particular would enhance the usefulness of the data collected considerably:

First, the scanning system should be calibrated with nonradioactive blanks having a range of densities approximating those of cores processed.

Second, some means for determining the energy spectra of the gamma radiation of the cores should be incorporated with the system.

Also, because of the disturbing effect of drilling and coring on recovered materials, an in-hole gamma ray logging program is strongly recommended.

ACKNOWLEDGMENTS

The author is grateful to Rudolph H. Beiri, Minoru Koide and Sachio Yamamoto who critically read the manuscript and offered a number of suggestions.

REFERENCES

American Petroleum Institute, 1959. *Recommended Practice for Standard Calibration and Form for Nuclear Logs.* New York (American Petroleum Institute).

Arrhenius, G. and Goldberg, E. O., 1955. Distribution of radioactivity in pelagic clays. *Tellus.* **7**, 226.

Arrhenius, Gustaf, 1963. Pelagic sediments. **In** *The Sea.* New York (John Wiley and Sons).

Arrhenius, G. *et al.*, 1957. Localization of radioactive and stable heavy nuclides in ocean sediments. *Nature.* **180**, 85.

Belknap, W. B., Dewan, J. J., Kirkpatrick, C. V., Motts, W. E., Pearson, A. J., and Rabson, W. R., 1966. A.P.I. calibration facility for nuclear logs. *A.P.I. Res. Paper.* **33** (Revised).

Bernat, Michel and Goldberg, E. D., 1969. Thorium isotopes in the marine environment. *Earth and Planetary Science Letters 5.* Amsterdam (North-Holland Publishing Co.), 308.

Chenouard, Lydie and Lalou, Claude, 1969. Gamma-Ray spectrometry as a tool for a rapid investigation of detritic cores. *J. Sediment Petrol.* **39** (4), 1477.

Chow, Tsaihwa, Tatsumoto, M. and Patterson, C. C., 1962. Lead isotopes and uranium contents in experimental Mohole cores (Guadalupe Site). *J. Sediment. Petrol.* 866.

Dixon, W. J. and Massey, Jr., F. G., 1957. *Introduction to Statistical Analysis.* New York (McGraw-Hill Book Co., Inc.).

Evans, H. B. and Lucia, J. A., 1970. Natural gamma radiation sources. **In** MNA Peterson *et al., Initial Reports of the Deep Sea Drilling Project, Volume II.* Washington (U. S. Government Printing Office).

Frielander, Gerbardt, Kennedy, Joseph and Miller, Julian, *Nuclear and Radio Chemistry.* New York (John Wiley and Sons).

Gealy, E. L. and Gerard, R. D., 1970. *In-situ* petrophysical measurements in the Caribbean. **In** Bader, R. G. *Initial Reports of the Deep Sea Drilling Project, Volume IV.* 1970, Washington (U. S. Government Printing Office).

Goldberg, E. D., 1954. Marine geochemistry, 1. chemical scavengers of the sea. *J. Geol.* **62**, 249.

Goldberg, E. D. and Arrhenius, G. O. S., 1958. Chemistry of Pacific pelagic sediments. *Geochim. Cosmochim. Acta.* **13**, 153.

Haglund, D. S., Friedman, G. M. and Miller, D. S., 1969. The effect of fresh water on the redistribution of uranium in carbonate sediments. *J. Sediment. Petrol.* **39** (4), 1283.

Heath, Russel, 1964. Scintillation spectrometry, gamma ray spectrum catalog. *At. Energy Commiss., Res. Develop. Rept. #IDO-16880-1.*

Kaufman, A., 1969. The Th^{232} concentration of surface ocean water. *Geochim. Cosmochim. Acta.* **33**, 717.

Koczy, F. F., 1954. Geochemical balance in the hydrosphere. **In** *Nuclear Geology*. H. Faul (Ed.) New York (John Wiley and Sons, Inc.), 120.

Koczy, F. F., Picciotto, E., Paul, G. and Wilgain, S., 1957. Mesure des isotopes du thorium dans l'eau de mer. *Geochim. Cosmochim. Acta.* **11**, 103.

Koczy, F. F., 1958. Natural Radium as a tracer in the ocean. *Proc. 2nd Intern. Conf. Peaceful Uses At. Energy*. **18**, 351.

Koczy, F. F., 1966. Age determination in sediments by natural radioactivity. **In** *The Sea*. New York (Interscience Publishers), **3**.

Ku, Teh-Lung and Broecker, W. S., 1969. Radiochemical studies on manganese nodules of deep-sea origin. *Deep-Sea Res.* **16**, 625.

Maxwell, A. E. *et al.*, 1970. Explanatory Notes. **In** *Initial Reports of the Deep Sea Drilling Project, Volume III.* Washington (U. S. Government Printing Office) 11.

Moore, W. S., 1969. Measurement of Ra^{228} and Th^{228} in sea water. *J. Geophys. Res.* **74** (2).

Scott, M. R., 1968. Thorium and uranium concentrations and isotope ratios in river sediments. *Earth and Planetary Science Letters 4.* 245.

Slack, T. and Way, K., 1959. Radiations from radioactive atoms in frequent use. *U. S. At. Energy Commiss., Washington, D. C.*

Turekian, Karl K., 1964. The marine geochemistry of strontium. *Geochim. Cosmochim. Acta.* **28**, 1479.

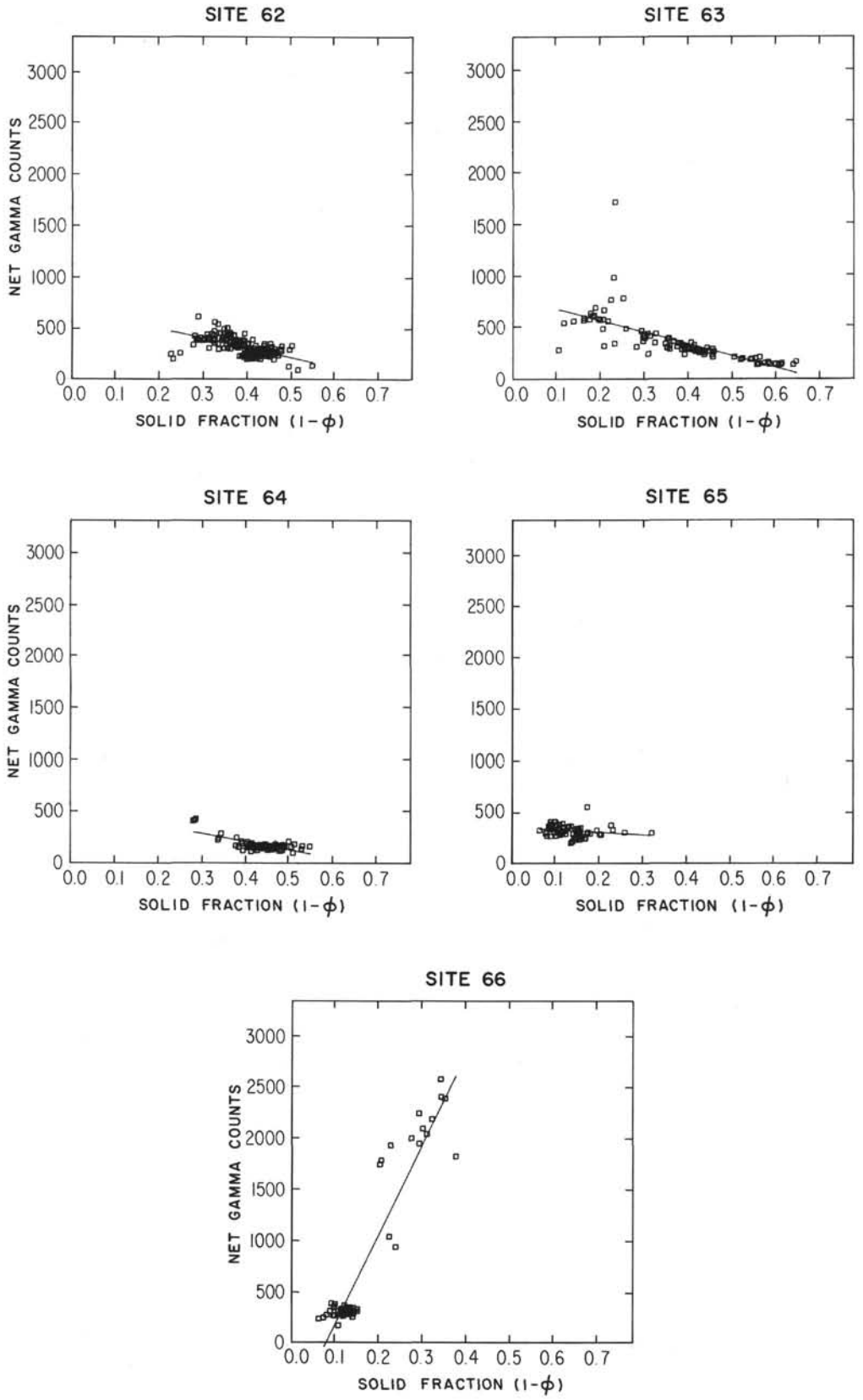

Figure 7. *Relationships between natural gamma radiation and net solid fraction for all sections taken at Sites 62, 63, 64, 65 and 66.*

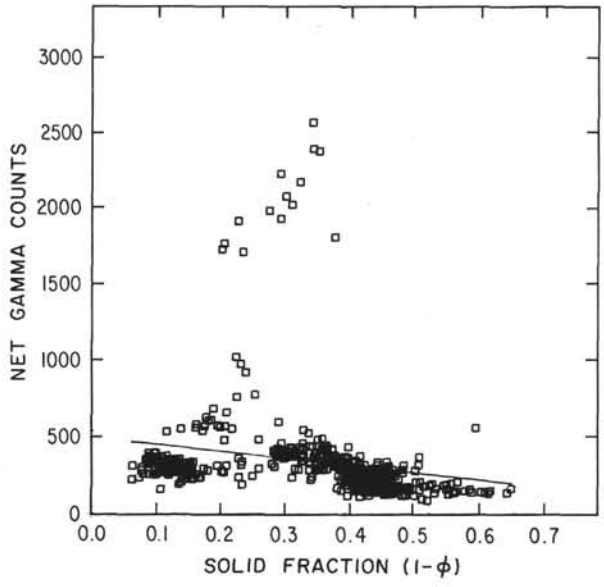

Figure 8. *Relationships between natural gamma radiation and net solid fraction for all sections taken at Sites 62 through 66: composite.*

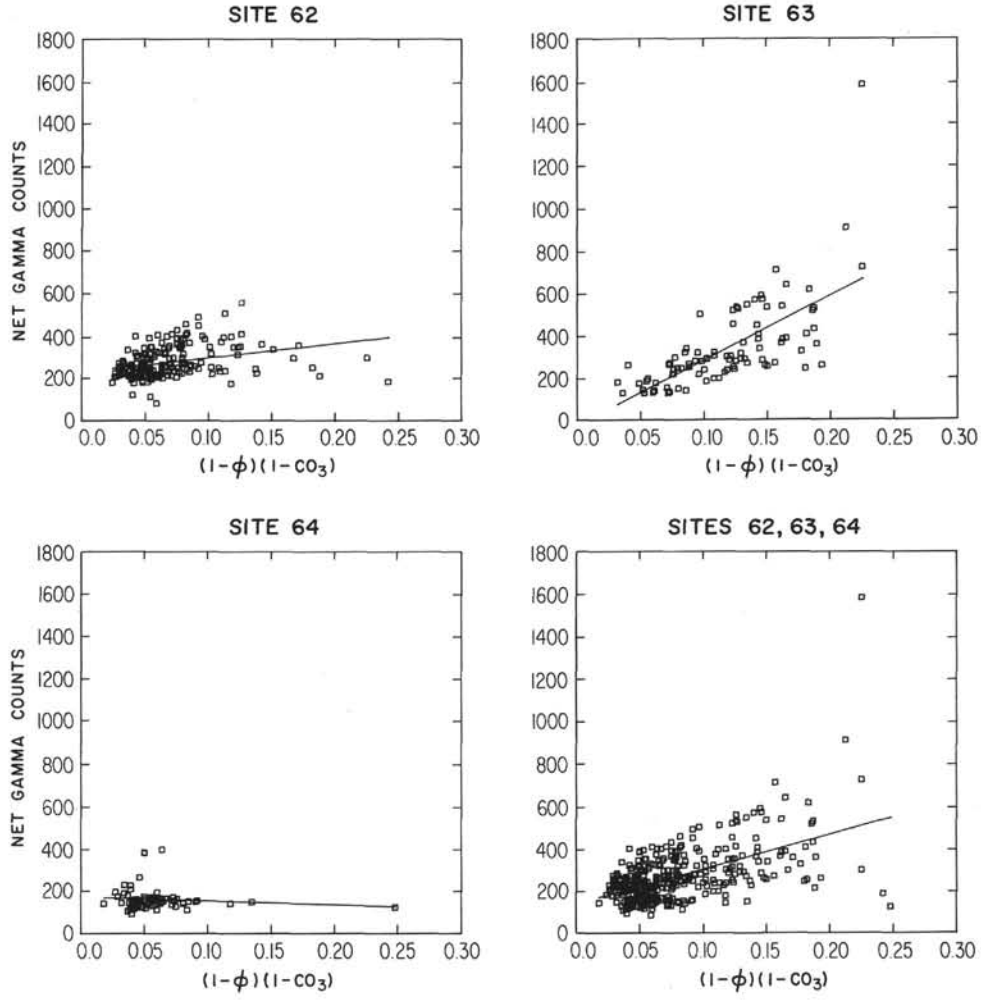

Figure 9. *Relationship between natural gamma radiation and net noncarbonate solid fraction for all sections taken at Sites 62, 63 and 64.*

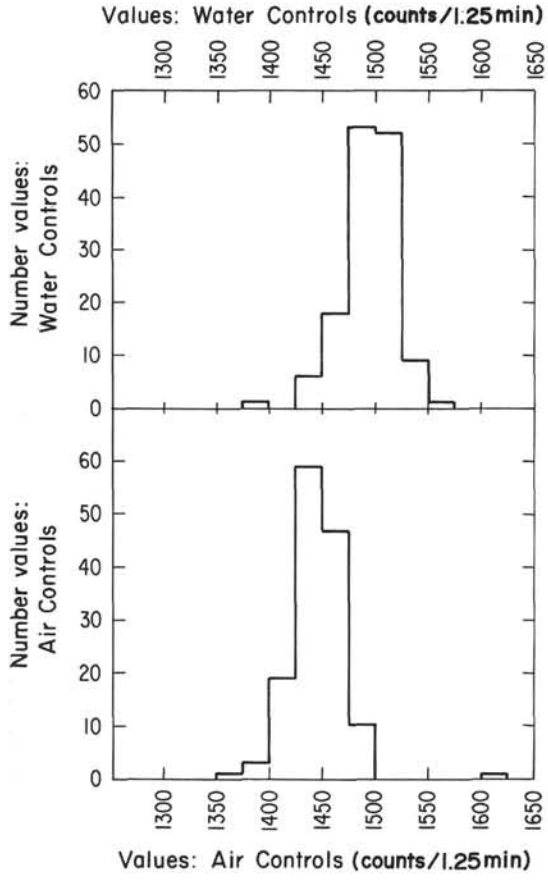

Figure 10. *Distribution air and water controls for natural gamma radiation.*

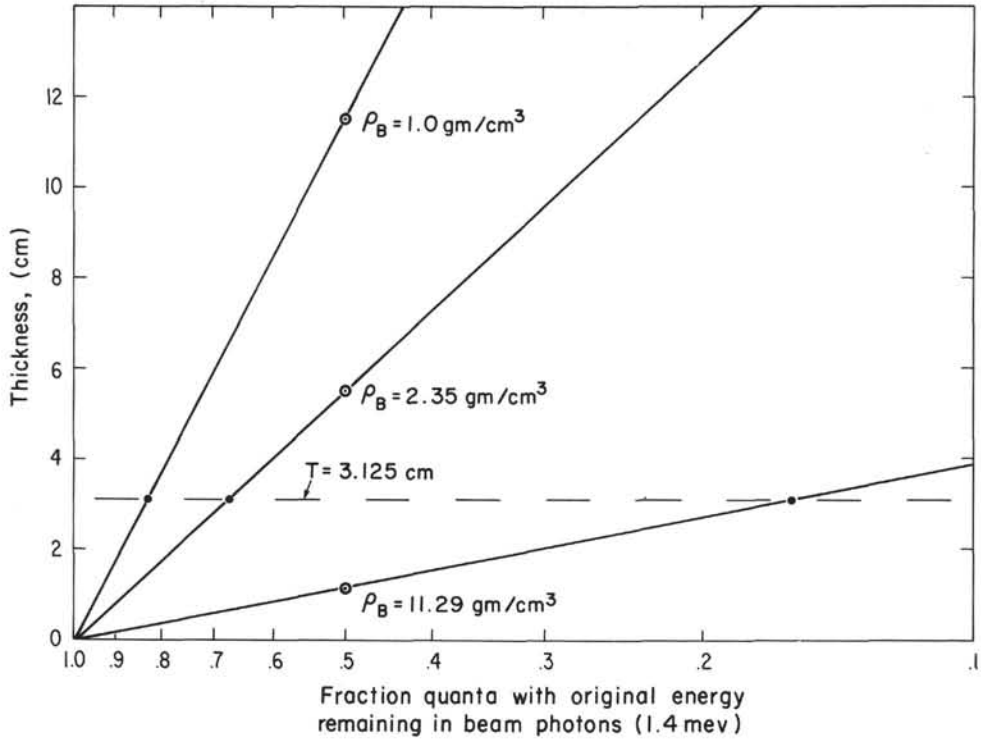

Figure 11. *Relationship between percentage original signal at 1.4 Mev remaining and half thickness.*

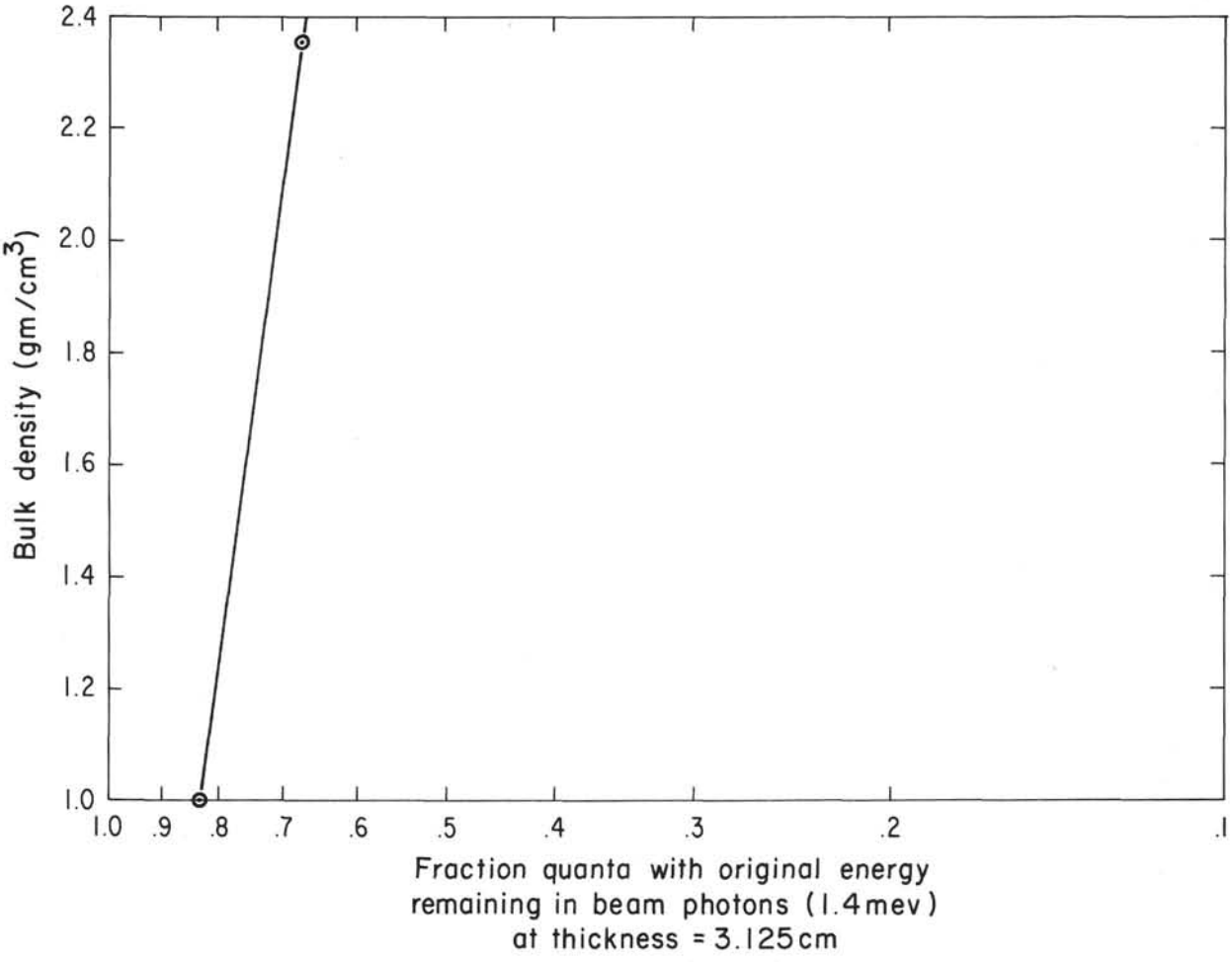

Figure 12. *Relationship between bulk density and percentage signal at 1.4 Mev remaining at* $T_{1/2}$ *= 3.125 centimeters.*